Relative Sea Level Trends for the Coastal Areas of Peninsular and East Malaysia Based on Remote and In Situ Observations

Simons, W.J.F.; Naeije, M.C.; Ghazali, Zaki ; Darani Rahman, Wan ; Cob, Sanusi ; Kadir, Majid; Bin Mustafar, M.A.; Din, Ami Hassan; Efendi, Joni Efendi; Noppradit, Prakrit

Important note
To cite this publication, please use the final published version (if applicable).
Please check the document version above.

Relative Sea Level Trends for the Coastal Areas of Peninsular and East Malaysia Based on Remote and In Situ Observations

Wim Simons [1,*], Marc Naeije [1], Zaki Ghazali [2], Wan Darani Rahman [2], Sanusi Cob [2], Majid Kadir [3], Asrul Mustafar [1,4], Ami Hassan Din [5], Joni Efendi [6] and Prakrit Noppradit [7]

[1] Astrodynamics and Space Missions, Space Engineering Department, Faculty of Aerospace Engineering, Delft University of Technology, 2629 HS Delft, The Netherlands

[2] Department of Survey and Mapping Malaysia, Jalan Sultan Yahya Petra, Kuala Lumpur 50578, Malaysia

[3] AFTech Construction Sdn. Bhd., No. 71-01, Jalan Pendidikan 4, Taman Universiti, Skudai 81300, Malaysia

[4] College of Built Environment, Universiti Teknologi MARA Perlis Branch, Arau 02600, Malaysia

[5] Geospatial Imaging and Information Research Group (GI2RG), Faculty of Built Environment and Surveying, Universiti Teknologi Malaysia, Johor Bahru 81310, Malaysia

[6] Center for Geodetic Control Network and Geodynamics, Geospatial Information Agency, Bogor 16911, Indonesia

[7] Coastal Oceanography and Climate Change Research Center, Faculty of Environmental Management, Prince of Songkla University, Songkla 90110, Thailand

* Correspondence: w.j.f.simons@tudelft.nl

Abstract: Absolute sea-level rise has become an important topic globally due to climate change. In addition, relative sea-level rise due to the vertical land motion in coastal areas can have a big societal impact. Vertical land motion (VLM) in Southeast Asia includes a tectonically induced component: uplift and subsidence in plate boundary zones where both Peninsular and East Malaysia are located. In this paper, the relative sea-level trends and (seismic cycle-induced) temporal changes across Malaysia were investigated. To do so, the data (1984–2019) from 21 tide gauges were analyzed, along with a subset (1994–2021) of nearby Malaysian GNSS stations. Changes in absolute sea level (ASL) at these locations (1992–2021) were also estimated from satellite altimetry data. As a first for Peninsular and East Malaysia, the combination ASL minus VLM was robustly used to validate relative sea-level rise from tide-gauge data and provide relative sea-level trend estimates based on a common data period of 25+ years. A good match between both the remote and in situ sea-level rise estimations was observed, especially for Peninsular Malaysia (differences < 1 mm/year), when split trends were estimated from the tide gauges and GNSS time series to distinguish between the different VLM regimes that exist due to the 2004 Sumatra–Andaman megathrust earthquake. As in the south of Thailand, post-seismic-induced negative VLM has increased relative sea-level rise by 2–3 mm/year along the Andaman Sea and Malacca Strait coastlines since 2005. For East Malaysia, the validation shows higher differences (bias of 2–3 mm/year), but this poorer match is significantly improved by either not including data after 1 January 2014 or applying a generic jump to all East Malay tide gauges from that date onwards. Overall, the present relative sea-level trends range from 4 to 6 mm/year for Malaysia with a few regions showing up to 9 mm/year due to human-induced land subsidence.

Keywords: relative sea-level rise; vertical land motion; tide gauge; satellite altimetry; plate deformation; GNSS

1. Introduction

Global climate change has highlighted the importance of monitoring sea level relative to the land (known as relative sea level—RSL) [1]. From the perspective of a country such as Malaysia, changes in RSL, and sea-level rise in particular, are important because they have significant impacts on the country's coastal communities and ecosystems [2–4].

Traditionally, RSL has been measured using data from tide gauges [5] with suitably long records, but gauges are frequently limited in number or are absent from many places of interest.

Alternative techniques are now available. Land movement, either through tectonic uplift or subsidence, are components of RSL [6] that can be measured as vertical land motion (VLM) using modern Global Navigation Satellite Systems (GNSS), whilst changes in the height of the sea surface (absolute sea level) can now be obtained from satellite altimetry (SALT). Taken together, VLM and SALT measurements combine to provide almost global cover for the estimation of RSL over the satellite epoch [7–9], which can then be used for comparison with tide-gauge records. Tide gauge (TG) stations that have been subject to tectonic vertical deformations or local human-induced subsidence (e.g., due to freshwater extraction or building infrastructure) will therefore exhibit higher or lower rates of RSL change compared to absolute sea-level change in the area.

Estimates of changes in RSL in Malaysia have hitherto been computed from TG data [5] employing a single linear regression model encompassing the entire data period. More recently, VLM in Malaysia (Peninsular Malaysia and East Malaysia (northern part of Borneo)) has also been monitored with a Global Positioning System (GPS) [10,11] and estimated as a single trend from varying time spans of GPS data between 1999 and 2011. A nearby study in the south of Thailand [6,12], on the same land mass as Peninsular Malaysia, has demonstrated that VLM has been affected by the inter- and post-seismic tectonic (deformation) phases of the (megathrust) seismic cycles in plate boundary zones associated with the subduction of the Australian and Indian plates below Sundaland. In particular, the 2004 Mw 9.2 Sumatra–Andaman earthquake [6,13] resulted in a marked change in the trend of VLM from 2005 onwards.

Tide-gauge data combined with local VLM information (1999–2004) and SALT has been used to study sea-level trends and variability around Peninsular Malaysia [14]. Over the period 1993–2009, Luu et al. [14] concluded that rates of absolute sea-level rise using tide-gauge data were similar to those from SALT data (~4.5 mm/year), later confirmed by [15,16]. This study, using VLM and SALT data as an alternative to TG data, was initially limited to TG locations in Peninsular Malaysia [14] and made use of (inter-seismic) VLM estimates from GPS data that predate 2005. A more recent study by Din et al. [17] estimated absolute sea-level rise (1993–2011) at TG stations across Malaysia by correcting the RSL (single trend) from tide-gauge records with VLM (single trend) estimates from GPS, Persistent Scatterer Interferometric Synthetic Aperture Radar (PS InSAR), and the SALT minus TG combination and reported an overall absolute sea-level rise of 4.47 ± 0.71 mm/year. While the rates observed were similar to those of previous studies, there were discrepancies in the results from the three VLM estimation methods with mostly similarities in their sign (overall subsidence). The latter implies that the RSL from TG records and the RSL from SALT minus VLM are not yet well matched and may need further refinement using both a larger time span and estimating split trends (<2005 and >2005) from both time series.

The aim of this work was to extend the earlier work and estimate RSL values over an extended time period at all the Department of Survey and Mapping Malaysia (DSMM) tide-gauge locations in both Peninsular and East Malaysia and then compare/validate the RSL results with the difference in absolute sea-level change (ASL) from satellite altimetry and vertical land motion (VLM) from the nearby DSMM continuous GNSS stations. For Peninsular Malaysia, we also distinguish (both for RSL and VLM) between the periods before and after the 2004 Mw 9.2 earthquake. Concurrently, the mean sea level was determined by Cob et al. [18] as part of defining a new height reference system for Peninsular Malaysia.

The tectonic setting of Peninsular Malaysia and East Malaysia is briefly discussed (Section 2), followed by the data and methodology to estimate the RSL (TG), ASL (SALT), and VLM (GPS) for both parts of Malaysia (Section 3). We then compare the TG results

with the RSL obtained from combining ASL and VLM at each TG location in Section 4. Finally, in Section 5, we summarize the main results and conclusions.

2. Study Area

Peninsular and East Malaysia (see the rectangular box in Figure 1 are part of the Sundaland tectonic plate (also known as the Sundaland block), which is surrounded by three main plates known as the Philippine Sea, Australian, and Indian plates [19,20]. As a result, the absolute horizontal (inter-seismic) motion of Malaysia follows that of the Sundaland plate and is about 3 cm/year in the ESE direction. However, the Sundaland block is a relatively small tectonic plate that is susceptible to pre-, co-, and post-seismic deformation. These three terms relate to the occurrence of megathrust earthquakes along the Sumatra–Andaman trench such as the Mw 9.2 Sumatra–Andaman earthquake at the end of 2004 [13]. As a result, Malaysia (and especially Peninsular Malaysia since it is situated closer to the Indian/Australian and Sundaland converging plate boundary) has, since the end of 2004, been undergoing both horizontal and vertical deformations, both instantly during the earthquake (co-seismic) and in the aftermath years until present (post-seismic) [12,21]. These (vertical) seismic deformation signals will also be present in the GNSS position time series of tide-gauge benchmarks.
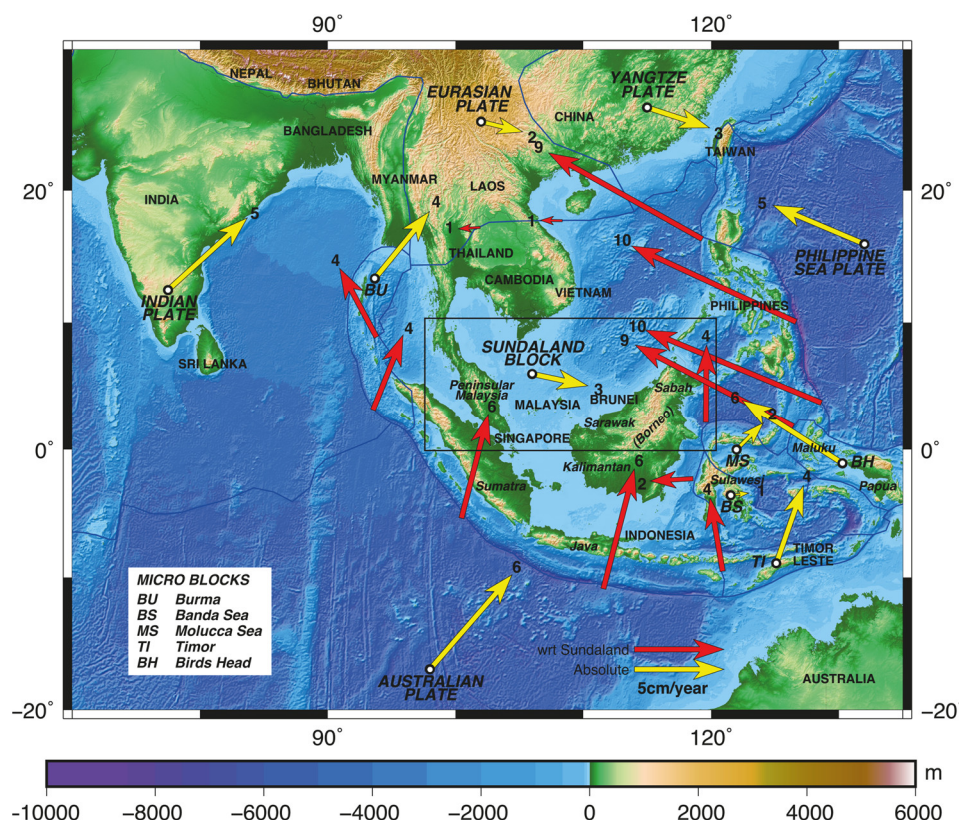
Figure 1. Tectonic setting of Southeast Asia with Peninsular Malaysia and East Malaysia (Sarawak and Sabah) being part of the Sundaland block along with the estimated relative and absolute horizontal velocities of plates and main/micro blocks that surround Sundaland (velocity magnitude in cm/year plotted near the head of the vectors). Approximate boundaries of plates (blue lines) are based on Bird [22]. Relative velocities on selected boundaries are with respect to Sundaland and calculated from Morvel56-NNR [23]. Absolute velocities are in IGS08 (ITRF2008) based on Sundaland motion from Mustafar et al. [24] and Morvel56-NNR plate vectors relative to Sundaland.

The study of the (vertical) tectonic motions of Phuket Island in South Thailand (north of Peninsular Malaysia) by Simons et al. [5] shows significant changes in (inter-, co-, and post-seismic) land deformation in the past 25 years. The region is located (similar

to the northwest of Peninsular Malaysia) at the edge of the Australian/Indian–Sundaland plate boundary deformation zone and has displayed significant deformations prior to, during, and after the 2004 megathrust earthquake. Although no vertical co-seismic position jumps were detected from this and the following 2005 Mw 8.6 Nias and 2012 Mw 8.6/8.2 Indian Ocean earthquakes, the vertical motion trend of Phuket started to change following the 2004 Mw 9.2 event. While the inter-seismic tectonic uplift motion up to the end of 2004 was quasi-linear (with only seasonal variations), the post-seismic tectonic subsidence phase follows an (approximately) exponential decay pattern starting shortly (about a month) after the earthquake. As a result, halfway through 2021, Phuket was located 8 ± 1 cm lower than it was before the earthquake and 11 ± 1 cm below its extrapolated inter-seismic vertical position if the earthquake had not occurred [25]. This is a significant short-time change in the vertical motion of the island. The vertical position (and associated RSL) changes after 2004 may hence also be relevant for Peninsular Malaysia, so that the RSL trend between 1994 and 2021 might not be linear, and the VLM and TG results may have to be split into an inter-seismic (1999–2004) and post-seismic (2005–2021) period for Peninsular Malaysia.

For East Malaysia (comprising the States of Sabah and Sarawak, as well as the federal territory of Labuan on Borneo in Figure 1) the tectonic setting is less complicated (being part of the stable core of the Sundaland plate) with the exception of the eastern part of Sabah in North Borneo. North Borneo is considered to be part of Sundaland near its eastern margins, close to highly active deformation zones bordering the southern Philippines and Sulawesi Islands in Figure 1. North Borneo is located at the junction between the North-West Borneo Trough and the Sulu Sea fold-and-thrust belt, to the north of the Celebes Sea. The way these two structures interact or connect is unfortunately still poorly understood. The region is characterized by low to moderate seismicity and most earthquakes have occurred at depths of less than 50 km. North Borneo nowadays seems to be slowly deforming in possibly different ways, either driven by gravity sliding and/or crustal shortening [24]. Therefore, the inter-seismic horizontal motions might differ from those of Peninsular Malaysia, and also, vertical motions in Sabah might regionally vary due to these ongoing tectonic processes. However, these motions should be stable over the analyzed period, and also the (post-seismic) impact of the Mw 9.2 Sumatra–Andaman earthquake will not be as significant here, as the co-seismic displacements were ~10 mm in western Sarawak down to ~5 mm in eastern Sabah [13]. This holds especially true for the VLM, which should not have been impacted, and exhibits a linear trend pattern over the analyzed period (1994–2021).

Based on the above information, the expected magnitude and pattern of the VLM in Peninsular and East Malaysia can be quantified. Tectonic plates do not move vertically but can deform at plate boundary zones. Significant uplift can only occur due to geophysical processes (NW Peninsular and Sabah). Human-induced land subsidence can occur due to groundwater extraction in populated areas with monuments on sedimentation layers (not on bedrock).

3. Data and Methodology

In this section, we present the methods used to estimate the RSL from the TG data, the ASL from the SALT data, and the VLM from the GPS data on Malaysia.

3.1. Relative Sea-Level Change from Tide-Gauge Data

We analyzed the tide-gauge RSL time series (1984–2019) from 12 Peninsular and 9 East Malaysian tide gauges (TG). The TGs are presented in Table 1 and Figure 2. We obtained the hourly tide-gauge data through AFTech from the Department of Survey and Mapping Malaysia (JUPEM) and reduced the data to monthly averaged mean sea-level (MSL) by averaging per tide gauge all hourly data available within a calendar month. This enables us to filter out most of the tidal constituents (especially diurnal and semi-diurnal) that should not be present in mean sea level. The actual number of hourly

data available in a month divided by the theoretical maximum number is taken as a measure of reliability: a ratio of 2/3 or more is taken as the criterion to constitute a valid monthly value. This is stricter than the 15-day rule used by the Permanent Service for Mean Sea Level (PSMSL). When we have a valid monthly value, the ratio is taken as a weight criterion in our data model fit. Apart from two stations, MYY and KCH, we analyzed the monthly averaged RSL time series without any special editing, such as introducing jumps, and we also did not apply an inverted barometer correction. It appeared that for MYY the data prior to 1991 needed to be corrected by adding an undocumented step of 82 cm, and after 1 January 2004, 10 cm needed to be subtracted to account for the 20 cm bias as reported by PSMSL and taking into account an approx. rise of 4.3 mm/year as deduced from our SALT minus VLM result (MYY and VLM at MIRI GPS station). For KCH, the data after 11 January 2010 were discarded automatically by our outlier detection scheme because of their erroneous behavior (which is also reported by PSMSL).

Table 1. The 21 tide gauges in Malaysia analyzed for the study: 12 in Peninsular Malaysia and 9 in East Malaysia. Given are the abbreviations, the geographic coordinates, the data period, the data completeness (in %), and the matching station ID number in the PSMSL database.

Area	Tide Gauge	Abbr.	Lon (°E)	Lat (°N)	Period	%	ID
Peninsular	Cendering	CHD	103.187	5.265	1985–2019	92.7	1592
	Geting	GET	102.107	6.226	1986–2018	96.3	1703
	Johor Bahru	JBH	103.792	1.462	1984–2015	93.0	248
	Kukup	KUK	103.443	1.325	1986–2020	98.0	1677
	Lumut	LUM	100.613	4.240	1985–2020	96.7	1594
	Pelabuhan Kelang	PTK	101.358	3.050	1984–2020	91.2	1591
	Pulau Langkawi	LAN	99.764	6.431	1986–2020	97.5	1676
	Pulau Penang	PEN	100.347	5.422	1985–2020	95.4	1595
	Pulau Tioman	TIO	104.140	2.807	1986–2020	94.8	1678
	Tanjung Gelang	NKP	103.430	3.975	1984–2020	96.9	1589
	Tanjung Keling	TGK	102.153	2.215	1985–2020	96.0	1593
	Tanjung Sedili	SED	104.115	1.932	1986–2020	95.2	1702
Sabah	Labuan	LBU	115.250	5.273	1996–2020	95.9	1879
	Lahat Datu	LDU	118.346	5.019	1996–2020	97.1	1877
	Kota Kinabalu	KKB	116.067	5.983	1987–2020	92.3	1733
	Kudat	KUD	116.844	6.879	1996–2020	88.6	1876
	Sandakan	SDK	118.067	5.810	1986–2020	93.8	1834
	Tawau	TWU	117.883	4.233	1987–2020	92.9	1734
Sarawak	Bintulu	BTU	113.064	3.262	1992–2019	85.0	1833
	Miri	MYY	113.974	4.401	1987–2016	65.1	1819
	Sejingkat	KCH	110.422	1.583	1996–2014	92.8	1893

In our analyses, we then applied an identical model fit as used for the satellite altimeter data (for which the reader is referred to the next section) to be able to directly compare the TG with the SALT result. As both TG and SALT clearly show signs of trends and periodic behavior, a simultaneous (robust) fit of linear and periodic signals is required: the trend estimate can be affected by the presence of periodic signals whenever the data span does not comprise an integer number of these periods.
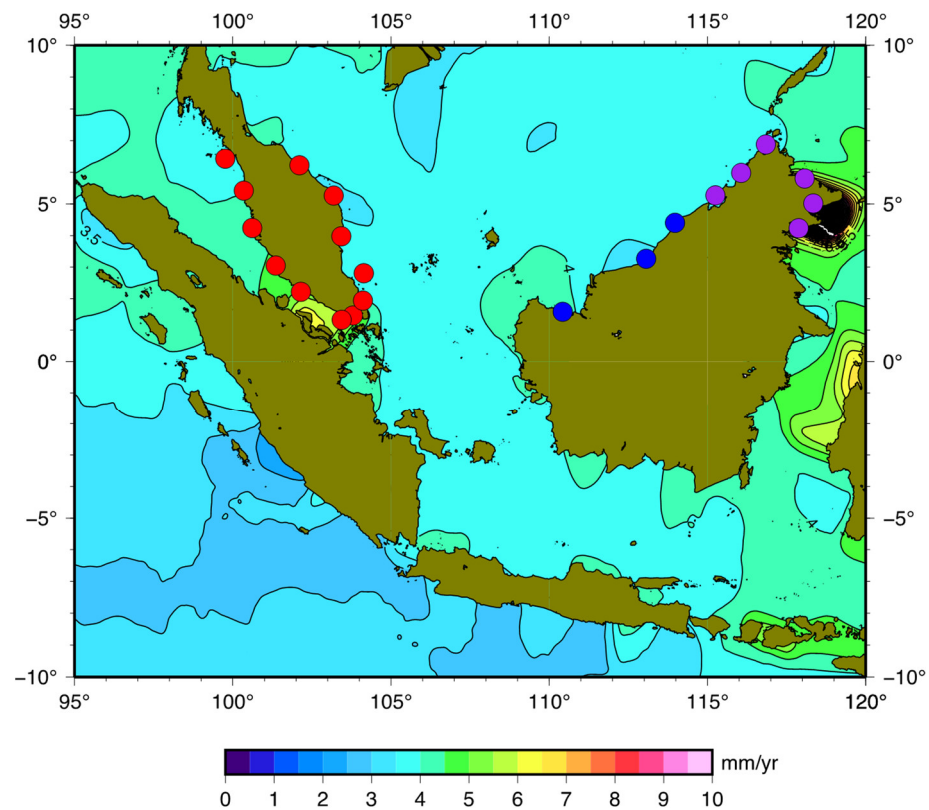
Figure 2. Geographical location of the 21 tide gauges, 12 in Peninsular Malaysia and 9 in East Malaysia. The colors indicate the trend in sea level anomaly from satellite altimetry for this region (yr=year). The *y*-axis is the latitude (N) and the *x*-axis is the longitude (E), both given in degrees.

Previous analyses indicate that the annual and semi-annual cycles are the most dominant ones. Simons et al. [5] also demonstrated that the tectonic setting of the region that contains Peninsular Malaysia can be affected by the seismic cycle of "nearby" megathrust earthquakes. Looking at the data of certain tide gauges, we concluded that for Peninsular Malaysia, there is a difference prior to and after 26 December 2004 when the 9.2 Mw Andaman–Sumatra Earthquake took place along the Sumatra Fault. This difference in the rate of vertical land motion affects both GNSS and TG data and indicates the transition from inter-seismic to post-seismic behavior. As the tide gauge measures RSL, it indirectly measures the opposite of the vertical land motion (vertically mirrored). As a first-order approach, for the tide-gauge stations located in Peninsular Malaysia, we included in our model fit different trend estimates prior to and after 2005 but also checked that no jumps were introduced at the point of the transition because there was no proof of that in our GNSS-based VLM estimates (piecewise linear regression). For the whole data period, we applied the same model for the annual and semi-annual cyclic periods. For the tide-gauge stations in East Malaysia, such a change in trend was not present and therefore was not needed and the model only includes bias, trend, and annual and semi-annual cycles for the entire data period. When fitting, we applied a 3σ outlier criterion, iteratively, to filter out extremes such as that in 1997, which was a low-sea-level event in the Indian Ocean due to the Indian Ocean Dipole (IOD) [26,27]. Results have not been corrected for Glacial Isostatic Adjustment (GIA), since its effect is small (<0.3 mm/year), but also cancels out in all the mutual comparisons between GPS, TG, and SALT.

Combining VLM from GNSS with satellite altimetry produces a value for relative sea level (SALT minus VLM), which can be compared with tide-gauge data and used as a proxy for tide-gauge measurements where none are available. In this way, all measurement techniques can be inter-validated and inter-calibrated [9,25,28]. This is valid for any combination of TG, SALT, and GNSS if we assume the TG is connected to the bedrock.

Any discrepancies then come from (un)charted contributions to local VLM and/or sea-level changes, such as groundwater extraction and local small-scale dynamics of tide–storm surge interactions.

Figure 3 provides two example solutions of our model fit (split at 26 December 2004) for station Chendering (CHD) in Kuala Terengganu. Before 2005, there is an RSL trend of 2.90 ± 0.33 mm/year (brown line); after 2005, this increases to 4.46 ± 0.46 mm/year (blue line). For station Tawau (TWU) the single trend line gives an RSL trend of 3.07 ± 0.34 mm/year. The green lines indicate the total model, which is trend plus periodic cycles (annual and semi-annual), the black dots represent the underlying data, and monthly averages and outliers are indicated by the red dots.
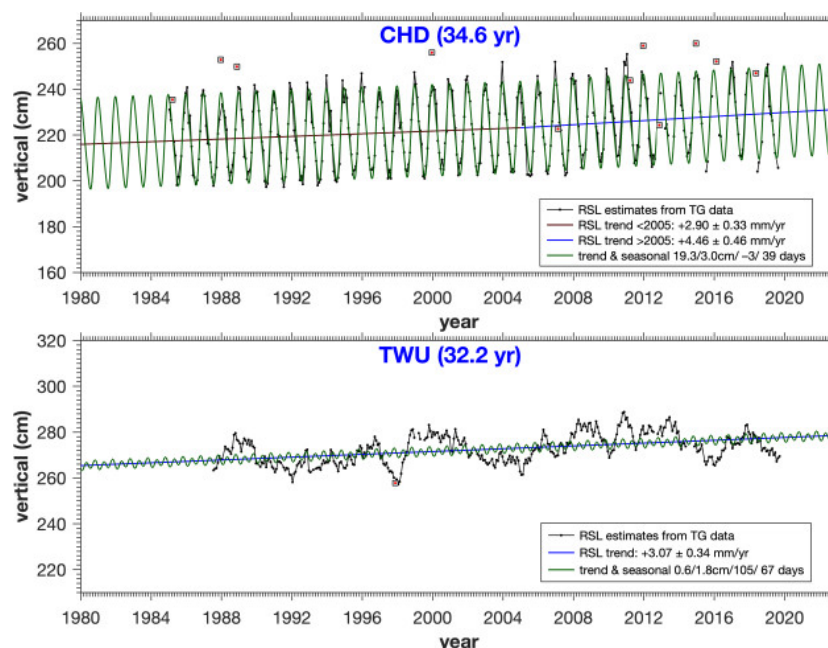

Figure 3. Relative sea level (RSL) trend and annual and semi-annual estimates from the tide-gauge time series (1984–2019) for CHD (Kuala Terengganu) in Peninsular Malaysia (split trend lines) and TWU (Tawau) in Sabah, East Malaysia. For each tide-gauge location, the vertical position time series is given along with the total observation period. The linear trend lines are shown in brown (<2005) and blue (>2005) (CHD split trend) and blue (>1988) (TWU single trend) with the modeled seasonal (annual) signal (green) superimposed. Monthly position outliers are marked in red. The tide-gauge trend estimates are given at a 95% (1.96 sigma) confidence level.

In the Supplementary Materials (Figures S1 and S2), the plots for all 21 tide gauges are shown, starting with the Peninsular Malaysia gauges with the 2005 split applied, followed by the plots for the tide gauges in East Malaysia, where no split was needed for our model fit. The total result of our model fit is given in Table 2 for Peninsular Malaysia and in Table 3 for East Malaysia.

Table 2. TG results for peninsular tide gauges (Peninsular Malaysia), before and after 2005. For the periodic cycles, the amplitude and phase are given where the latter is transformed to days after 1 January. The residual sigma is the std of the difference between data and model fit. Trend uncertainties are given at a 95% confidence level (1.96 sigma).

TG Station	Trend < 2005 (mm/year)	Trend > 2005 (mm/year)	Annual (cm/days)	Semi-Annual (cm/days)	Residual SD (cm)
LAN	2.23 ± 0.55	4.61 ± 0.69	8.91/139	6.60/41	6.06
GET	2.70 ± 0.47	5.56 ± 0.67	22.02/−1	3.90/29	5.00
PEN	2.50 ± 0.51	4.80 ± 0.71	7.97/135	6.72/39	5.97
CHD	2.90 ± 0.33	4.46 ± 0.46	19.28/−3	3.01/39	3.90

LUM	2.27 ± 0.50	3.60 ± 0.66	6.76/127	6.88/37	5.79
NKP	2.56 ± 0.29	5.05 ± 0.42	18.68/−4	2.37/39	3.61
PTK	1.57 ± 0.50	3.66 ± 0.72	6.24/116	7.10/40	6.16
TIO	2.18 ± 0.32	4.26 ± 0.40	16.93/−1	2.23/37	3.54
TGK	1.69 ± 0.47	3.31 ± 0.64	4.98/85	5.52/37	4.73
SED	2.23 ± 0.37	2.55 ± 0.45	17.60/−2	2.11/22	3.39
JBH	2.13 ± 0.27	7.84 ± 0.61	13.65/0	2.22/23	3.34
KUK	1.87 ± 0.38	7.97 ± 0.48	5.48/46	4.83/35	4.18

Table 3. TG results for Sabah and Sarawak (East Malaysia). No trend split was needed. For the periodic cycles, the amplitude and phase are given where the latter is transformed to days after 1 January. The residual sigma is the std of the difference between data and model fit. Trend uncertainties are given at a 95% confidence level (1.96 sigma).

TG Station	Trend (mm/year)	Annual (cm/days)	Semi-Annual (cm/days)	Residual SD (cm)
KCH [1]	−4.98 ± 0.34	9.57/1	1.02/8	3.03
BTU	2.52 ± 0.28	8.03/35	2.24/32	3.76
MYY [2]	4.84 ± 0.31	7.13/48	2.47/37	4.45
LBU	2.08 ± 0.40	7.73/53	3.33/32	4.79
KKB	3.82 ± 0.29	8.16/72	3.53/36	4.76
KUD	2.46 ± 0.40	8.77/73	3.08/29	4.78
SDK	2.75 ± 0.36	6.80/46	1.51/27	4.78
LDU	1.83 ± 0.47	2.53/93	1.53/58	5.61
TWU	3.07 ± 0.34	0.60/105	1.78/67	5.52

[1] KCH data after 11 January 2010 discarded because of erroneous behavior (also reported by PSMSL). [2] MYY data prior to 1991 has been corrected by adding an estimated step of 82 cm, and after 1 January 2004, 10 cm was subtracted to account for a 20 cm bias, as reported by PSMSL and accounting for an approx. rise of 4.3 mm/year deduced from the SALT−VLM results.

3.2. Absolute Sea Level Observed with Satellite Altimetry

Satellite altimetry is a well-founded space geodetic technique that enables the measurement of absolute sea level (ASL); that is, with respect to a reference ellipsoid, such as WGS-84 or IERS. For communities living near low-lying coasts and islands, however, it is the relative sea level (RSL) that is most important since this is the actual water level relative to the land. Altimeter observations do not contain information on land motion, such as uplift and subsidence in active tectonic regions, or subsidence that could result from soil compaction or groundwater extraction. Basically, they are unaffected by VLM, though they could be affected by a change in local gravity; however, that is assumed to be negligible. Though tide-gauge measurements directly measure relative sea level (as explained in the previous section), they suffer from inaccuracies related to (documented and undocumented) changes in the vertical reference benchmark, (human-induced) land subsidence by groundwater extraction, and sediment compaction if the tide gauge is not directly attached to the bedrock. As mentioned earlier, VLM and SALT provide an estimate of SALT−VLM as long as GNSS is a good indicator for all the contributors to land motion. We refer to Naeije et al. [25] and Trisirisatayawong et al. [29] for more details on the altimeter (and tide-gauge) data processing. In this section, we only review the main steps and the deviations from the original processing.

For the satellite altimeter data used in this study of absolute and relative sea level variations in the waters surrounding Malaysia, such as the Strait of Malacca and the South China Sea, we adopt the TU Delft/NOAA/EUMETSAT Radar Altimeter Database System (RADS) [30]; http://rads.tudelft.nl (accessed on 1 January 2023) and https://github.com/remkos/rads (accessed on 1 January 2023). RADS delivers a consistent and continuous observing database that has a complete backlog of all available

low-resolution mode (LRM = 1 Hz) altimeter observations since the 1990s. The measurement principle is straightforward: the altimeter emits a microwave pulse and clocks the reception of the echo reflected from the sea surface. Then, by applying corrections for, amongst other things, atmospheric refraction, the orbital height of the altimeter referenced to the reference ellipsoid minus this measured reflection distance directly gives sea level with respect to that same ellipsoid. So, this provides a measurement of the absolute sea level, which can be further reduced to dynamic topography by subtracting a geoid model or to a sea level anomaly (SLA) by subtracting a mean sea surface model. The latter is used in our analyses.

From RADS, we only used data from the altimeter reference missions TOPEX/POSEIDON, Jason-1, Jason-2, and Jason-3 considering the time frame of August 1992 up to and including December 2021. This ensured that we had identical temporal and spatial sampling conditions throughout the total period and the most reliable data. Figure 4 shows the study area with our tide gauges and the altimeter satellite tracks from these reference missions used in our study. It should be noted that the altimeter sampling period is different (a measurement along-track every second, with the track repeated every 10 days) from the sampling of tide gauges (high-frequency, one location).
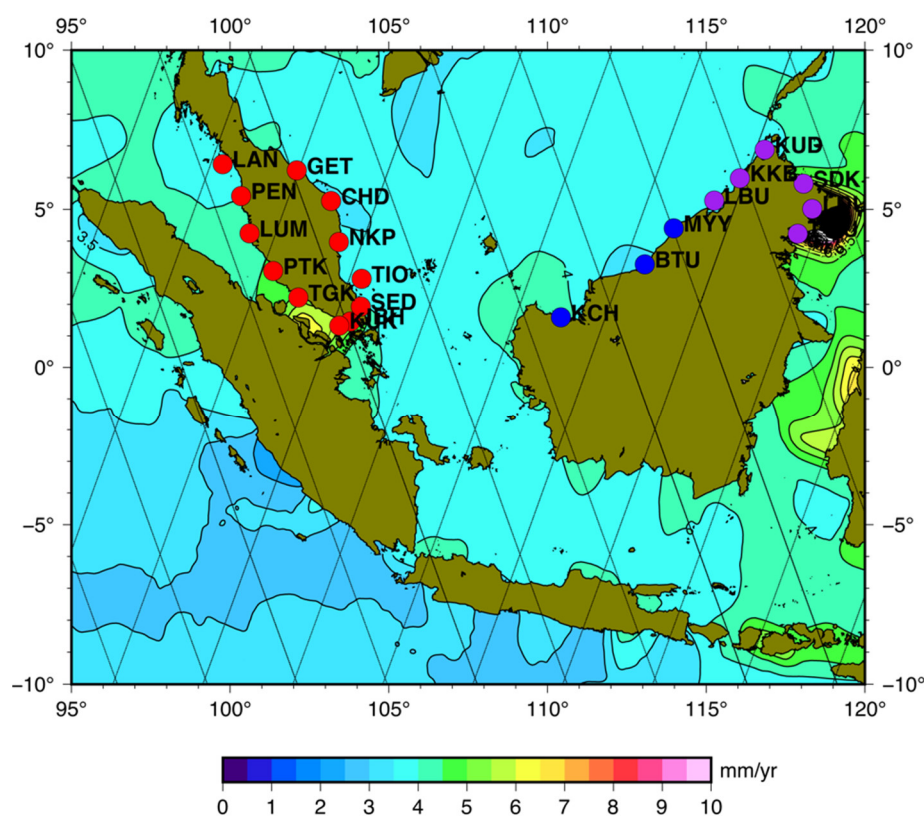

Figure 4. The Malaysian study area with the tide-gauge locations and, superimposed, the satellite tracks of the reference missions such as TOPEX and the Jasons. Again, in the background, we see the geographical distribution of the trend of the absolute sea level w.r.t the mean surface model (sea level anomaly SLA). The *y*-axis is the latitude (N) and the *x*-axis is the longitude (E), both given in degrees.

The altimeter data are already validated and calibrated in RADS and can easily be combined without suffering from discontinuities over time, going from one satellite altimeter mission or phase to the other. As mentioned before, we obtain the altimetric sea level anomaly (SLA) by subtracting the instrument-corrected measured range from the orbital height and subtracting the required corrections, such as corrections for dry and wet troposphere, ionosphere, high-frequency dynamic atmosphere, ocean tide, ocean tide loading, solid Earth tide, pole tide, sea state bias, and mean sea surface (model). The

static inverse barometer correction was not applied because this is also not applied to the tide-gauge data. On the other hand, like the tidal contributions, the high-frequency component of the dynamic atmosphere must be corrected because it aliases into the altimeter data at considerably longer wavelengths (a result of under-sampling). The high-frequency dynamic atmosphere correction is not needed for the tide gauges because it is averaged out in the monthly means (no under-sampling). For the corrections, we used the RADS default values (for details, consult the RADS data manual at https://github.com/remkos/rads (accessed on 1 January 2023)). The only deviation is that we edited out SLAs between −1 m and +1 m in order to discard erroneous data that were either too close to the coast, and thus suffering from land contamination in the footprint, or had poor tidal modeling or poor mean surface modeling.

For our study area, bounded by 95 and 120 degrees longitude and −10 and +10 degrees latitude, we browsed sequentially through our database and collected all altimeter data from the altimeter reference missions in a small circular region (radius 1.5 degrees) around the location of the tide gauge with which we want to compare the ASL/SLA, so that is, in total, 21 time series with a reoccurrence of a lump of 1Hz data every 10 days (which, as mentioned before, is the repeat orbit of the altimeter satellites used). We originally started our analysis by constructing monthly average SLA grids from the altimeter data but deviated from this approach to keep the data un-interpolated as long as possible, so as not to introduce any interpolation errors and/or lose track of data quality. Having the raw data in time series for each of the tide gauges enabled a much more reliable outlier detection. Data that were very close in time (seconds apart) were combined, and their time, height, and location were averaged.

The ASL trend was then obtained by simultaneously fitting a bias, trend, and two periodic cycles (annual and semi-annual) to the SLA time series for each of the TG locations. Again, an iterative 3σ outlier criterion was applied for the model fit to filter out the extremes (as with the TG data). The SALT results were also not corrected for GIA, since its effect on ASL is, again, small and cancels out in the comparisons with TG RSL and GNSS VLM. For the total ASL, the mean sea surface model must be added to the SLA to arrive at sea level with respect to the reference ellipsoid. As mentioned earlier, we did not apply a split in trends at the 26 December 2004 earthquake epoch because the ASL is (assumed to be) unaffected by land motion.

Figure 5 shows an example of our model fit for the ASL. For comparison reasons, we again chose the location of the CHD and TWU stations shown in Figure 3. There is an ASL trend of 3.52 ± 0.24 mm/year and 4.49 ± 0.23 mm/year (blue lines), respectively, for CHD and TWU from 1992 to 2021. The green line indicates the total model, which is trend plus periodic cycles (annual and semi-annual), the inter-connected black dots represent the underlying altimeter data (our raw time series in the vicinity of the tide-gauge location), and outliers are shown as red dots.

In the Supplementary Materials (Figures S3 and S4), the plots for the ASL from altimetry at all 21 TG locations are shown, starting with the Peninsular Malaysia TGs followed by the plots for the TG locations in East Malaysia. Table 4 gives the overview of the altimeter results for Peninsular Malaysia and Table 5 for East Malaysia.
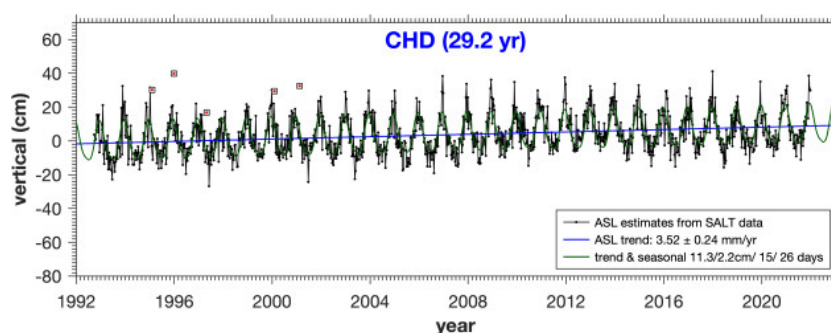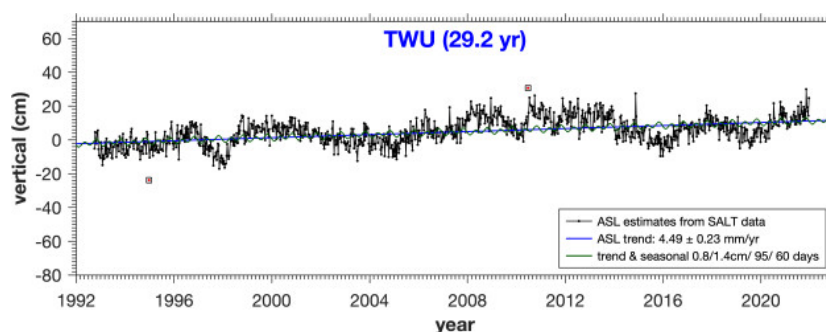
Figure 5. Absolute sea-level trend and annual and semi-annual cycle estimates from the satellite altimetry time series (1992–2021) for CHD (Kuala Terengganu) in Peninsular Malaysia and TWU (Tawau) in Sabah, East Malaysia. For each tide-gauge location, the vertical position time series is given along with the total observation period. The reference vertical position is at the start of the satellite altimetry time series in 1992. The linear trend lines are given in blue with the modeled seasonal (annual and semi-annual) signal (green) superimposed on it. Outliers are marked in red. The absolute sea-level trend estimate is given at a 95% (1.96 sigma) confidence level.

Table 4. ASL trend results (1992–2020) from SALT for the TG locations in Peninsular Malaysia. The average distance of the altimeter along-track data to the TG station location is given in the 2nd column. For the periodic cycles (annual and semi-annual), the amplitude and phase are given where the latter is transformed to days after 1 January. The residual sigma is the SD of the difference between data and model fit. The ASL trend estimates are given at a 95% (1.96 sigma) confidence level.

TG Station	SALT Station (km)	ASL Trend (mm/year)	Annual (cm/days)	Semi-Annual (cm/days)	Residual SD (cm)
LAN	45	4.08 ± 0.28	7.98/143	7.26/37	8.24
GET	62	3.68 ± 0.26	18.99/−4	3.34/30	7.56
PEN	98	4.03 ± 0.29	8.57/144	7.16/38	8.53
CHD	38	3.52 ± 0.24	11.31/15	2.23/26	7.15
LUM	34	4.30 ± 0.31	7.16/137	6.96/38	9.07
NKP	77	3.66 ± 0.26	14.40/5	2.58/29	7.72
PTK	37	4.73 ± 0.35	5.90/120	6.55/37	10.10
TIO	40	3.67 ± 0.27	15.77/2	2.62/30	8.01
TGK	4	4.08 ± 0.27	6.14/100	6.97/25	7.78
SED	16	4.88 ± 0.29	12.41/7	2.83/34	8.53
JBH	37	5.12 ± 0.31	8.91/15	3.37/36	9.19
KUK	6	4.73 ± 0.34	6.70/21	3.00/30	9.95

Table 5. ASL trend results (1992–2020) from SALT for the TG locations in East Malaysia (Sarawak and Sabah). The average distance of the altimeter along-track data to the TG station location is given in the 2nd column. For the periodic cycles (annual and semi-annual), the amplitude and phase are given where the latter is transformed to days after 1 January. The residual sigma is the SD of the difference between data and model fit. The ASL trend estimates are given at a 95% (1.96 sigma) confidence level.

TG Station	SALT Station (km)	Trend (mm/year)	Annual (cm/days)	Semi-Annual (cm/days)	Residual SD (cm)
KCH	144	4.18 ± 0.19	9.97/13	2.70/25	5.67
BTU	66	3.43 ± 0.23	7.50/36	3.13/25	6.69
MYY	62	3.66 ± 0.18	7.34/45	3.24/26	5.12
LBU	144	3.64 ± 0.27	8.00/71	4.07/31	7.82
KKB	56	3.88 ± 0.24	7.91/70	3.86/30	6.91
KUD	29	3.92 ± 0.22	7.63/71	3.66/29	6.49
SDK	103	4.34 ± 0.20	5.25/85	1.78/42	5.93

| LDU | 39 | 4.76 ± 0.20 | 3.66/80 | 1.41/46 | 5.79 |
| TWU | 58 | 4.49 ± 0.23 | 0.83/95 | 1.45/60 | 6.71 |

3.3. Reference Frame and Vertical Land Motion (VLM)

The vertical land motion (VLM) at a set of GNSS stations in Malaysia was analyzed because, in combination with the absolute sea level (ASL) from satellite altimetry, it provides an independent estimation of relative sea level (RSL) at coastal GNSS stations that can be compared with the RSL of tide-gauge (TG) stations.

3.3.1. MASS/MyRTKNet Subset Network Selection

A subset of the Malaysian Active GPS (MASS) and GNSS MyRTKNet networks was analyzed over the period of 1994–2021. The MASS network has been operational since the end of 1999 and subsequently was merged into MyRTKNet from 2005 onwards. The inclusion of the GPS MASS stations is important as it allowed us to analyze a time period of up to 27 years, since the KUAL point originally was a station of the Geodynamics of South and South East Asia (GEODYSSEA) 1994–1998 EU-ASEAN project [31]. This also included another GEODYSSEA station TAWA near the MASS MTAW station in Tawau in Sabah, East Malaysia. Both the KUAL and TAWA stations have been measured by DSMM in campaign style prior to 1999, and TAWA was also measured until 2000 when the MTAW station already was operational. The majority of the MASS stations later became part of MyRTKNet, although some stations were eventually replaced with nearby new MyRTKNet stations. For the majority of these stations, there was also data overlap during the station transitions so that an accurate tie between the stations can be computed. Hence, it is possible to compute (station-combined) long GPS time series (1999–2021) for 18 MASS/MyRTKNet locations and for KUAL and TAWA/MTAW even since 1994.

MyRTKNet (2005–2021) currently comprises ~100 stations. For the selection of a sub-network to be included in the GNSS data analysis, the following criteria were used:

- Close to tide gauge (TG) stations;
- Close to (decommissioned) MASS stations (combined position time series);
- Additional inland stations (which can be used as stable reference stations);
- Early MyRTKNet stations only (2005–2007) (to construct long position time series);
- Evenly distributed throughout both Peninsular and East Malaysia.

In addition, also one IGS station, NTUS (1997–2021) (Singapore), and 4 stations (CNAT, CBAS, CPUT, and CNAU from 2014 to 2021) from the Indonesian InaCORS network operated by the Geospatial Information Agency (BIG, formerly known as BAKOSURTANAL) on Kalimantan/Borneo close to Sarawak and Sabah, were included, as well as the TU Delft station MKNB (2013–2021) on Mount Kinabalu.

For Peninsular Malaysia, in total, 29 MASS/MyRTKNet stations evenly distributed at 20 locations (Figure 6) were selected, including those located near the 12 TG station locations. At 5 locations (GETI/GET2, KUAN/PEKN, KTPH/UPMS, SEGA/SEG1, and UTMJ/JHJY), the MASS and MyRTKNet stations were combined into a single GPS position time series that has the name of the (newer) MyRTKNet station. At 2 locations (MERS/MRSG and TGRH/SDLI), the MyRTKNet stations were combined into a single GPS position time series that has the name of the (newer) MyRTKNet station. The station KUAL has the longest position time series (1994–2021) due to including the GEODYSSEA (1994–1998) GPS campaign data.

For East Malaysia, 17 MASS/MyRTKNet stations and 1 GEODYSSEA station at 12 locations were selected (Figure 7), including those located near the 9 TG locations. At 6 locations (KUCH/UMAS, SIBU/SIB1, BINT/BIN1, LABU/LAB1, KINA/UMSS, TAWA/MTAW), the MASS and MyRTKNet stations were combined into a single GPS position time series that has the name of the (newer) MyRTKNet station. At Tawau, the GEODYSSEA (TAWA) and MyRTKNet station (MTAW) were combined into a single

GPS position time series that has the name of the (newer) MyRTKNet station and has the longest position time series (1994–2021) due to including the GEODYSSEA (1994–2000) GPS campaign data.

Therefore, in total, the GPS data of 47 MASS/MyRTKNet/GEODYSSEA stations at 32 locations were analyzed. In addition, the GPS data of 1 IGS, 4 BIG, and 1 TUDelft were also analyzed at 6 locations. At 2 locations, 2 MyRTKNet stations were analyzed (ARAU/UUMK and USMP/BABH), meaning that, in total, 40 (single/combined) GPS time series were computed.

Figure 6. Location of 29 MASS/MyRTKNet stations at 20 locations (of which 12 are near the tide gauges) in Peninsular Malaysia. Shown also are the 11 tide-gauge benchmarks (in red, located below GETI/GET2). The tide-gauge benchmark at Johor Bahru unfortunately was lost during harbor reconstruction. Additionally, the other 60+ MyRTKNet stations currently operated by DSMM are shown (yellow open stars). The purple dot shows the NTUS station in Singapore which is part of the International GNSS Service (IGS) network. Yellow indicates still active and orange discontinued stations. Image made with Google Earth Pro.

Figure 7. Location of 17 MASS/MyRTKNet and 1 GEODYSSA stations at 12 locations (of which 9 are near the tide gauges) in East Malaysia. Shown also are the 8 tide-gauge benchmarks (in red). Additionally, the 20+ other MyRTKNet stations (including 3 off-shore) currently operated by

DSMM are shown (yellow open stars). The purple dots show the Indonesian InaCORS stations (CNAT, CBAS, CPUT, and CNAU) in the Indonesian part of Borneo (Kalimantan) as well as the TU Delft station MKNB on Mount Kinabalu in Sabah. Yellow indicates still active and orange discontinued stations. Image made with Google Earth Pro.

3.3.2. GPS Data Analysis

The GPS data analysis period spans the period of November 1994 until December 2021, where, from January 1999 onwards, continuous MASS and later MyRTKNet GPS data were processed. From 1994 to 1999, only GEODYSSEA and DSMM campaign data were included. Dual frequency GPS data from 47 MASS/MyRTKNet/GEODYSSEA stations were processed along with additional data from TU Delft (station MKNB), BIG (stations CNAT, CBAS, CPUT, and CNAU), and the IGS (station NTUS). The inclusion of these additional GPS data is not compulsory, but it allows for additional VLM estimates in and near both Peninsular and East Malaysia. Additionally, the stations can improve the GPS position solutions due to enhanced (regional) phase ambiguity fixing.

We made use of the (zero-differencing) scientific GIPSY-OASIS II software (version 6.4) [32] to process the GPS data (with a 30 s sampling rate) in the 2014 global reference frame solution of IGS (IGS14) [33], which is based on the International Terrestrial Reference Frame 2014 (ITRF2014) [34]. We modified the Jet Propulsion Laboratory (JPL) software package in order to include GPS data from the new block III GPS satellites that have become operational since 2019 (GPS 74–78). To derive precise daily coordinate results, the Precise Point Positioning (PPP) method with (regional network) ambiguity fixing [35] was used. The precise ephemeris of satellites along with Earth rotation parameters (non-fiducial style, IGS14) acquired from JPL enable the consistent derivation of highly accurate daily absolute GPS positions over the entire analyzed period.

Non-fiducial (i.e., no pre-constrained reference station positions) daily position solutions were computed with GIPSY in an identical way as described in Simons et al. [5]. To align these solutions with the IGS14, daily transformation parameters (X-files, provided by JPL) were applied to all positions. Finally, weekly averaged station positions were computed. This averaging was performed to screen for any outliers, thereby improving the reliability of the coordinate solutions. The daily repeatabilities (Weighted Root Mean Square (WRMS)) of the weekly averaged station coordinates from 1994 to 2021 (all in mm) are 1.2/1.3/4.7 (47 MASS+MyRTKNet+GEODYSSEA stations), 1.1/1.4/4.0 (NTUS), 1.3/1.2/6.2 (MKNB), and 1.3/1.5/5.8 (BIG stations) in, respectively, the north, east, and vertical position components. The above WRMS values also give a direct indication of the absolute accuracy of the daily station coordinates in IGS14 since all daily station positions were directly mapped in this global reference frame with the JPL X-file technique.

A few MASS/MyRTKNet stations have higher WRMS (KUCH/TGPG) due to temporary daily GPS data quality issues. Some stations temporarily had weak daily position solutions due to long-term GPS data issues (BEHR, SIB1, LAB1, and UMSS). Moreover, there was a big data gap (~6 months) in the first half of 2007 for many stations. There were also stations renamed and re-located in the analyzed period: MERS/MRSG (renamed in 2016), TGRH/SDLI (moved 25 km in 2015 + renamed), SEMP (moved 5 km in 2015), and KUDA (moved 2 km in 2020 after 5-year data gap). Overall, the daily GPS positioning results from the MASS and MyRTKNet networks suggest that their VLM can be used to monitor nearby tide-gauge station (vertical) motion changes at the mm/year level.

3.3.3. GPS Velocity Estimation

The weekly averaged coordinate solutions in the IGS14 were then used to estimate the velocities of all stations by applying a 3D linear regression method to the position time series. First. unfiltered GPS position time series were computed (both absolute and detrended ones) in order to identify height position jumps and (extreme) weekly position

outliers. The total time period spanned by the GPS observations is the longest at stations KUAL (Kuala Terengganu) and MTAW (Tawau) for the new KTPH station (27.1 years including the GEODYSSEA campaign style observations between 1994 and 1998). The unfiltered 3D linear velocity estimates for stations KUAL and MTAW are given in Figure 8. For the velocity uncertainties, we used the method (2×WRMS/T) of Simons et al. [20], which makes use of the WRMS of the position misfits and the time period T of the observations to estimate the maximum possible tilt of the trend line with a confidence level of 99.999%. The latter results in higher (and more realistic) uncertainties than those given by the final statistics of the linear regression.

Although the horizontal position time series in Peninsular and East Malaysia have been (more significantly for Peninsular Malaysia) affected by major earthquake events (both by co- and post-seismic position changes since 26 December 2004), the vertical position time series of GNSS stations in Peninsular Malaysia (in the far field; 500–850 km away from the earthquake epicenters) remained undisturbed. They have only been affected by a non-linear pattern change (post-seismic tectonic subsidence) following the 2004 Mw 9.2 Sumatra–Andaman earthquake. Hence, this VLM trend-change phenomenon required additional attention when validating TG-relative sea-level change time series with the difference in absolute sea-level change time series from SALT and VLM. These should be compared over the same time periods (e.g., 1984–2005 and 2005–2020) since VLM in Peninsular Malaysia is different in these two periods (as will be shown in Section 4).
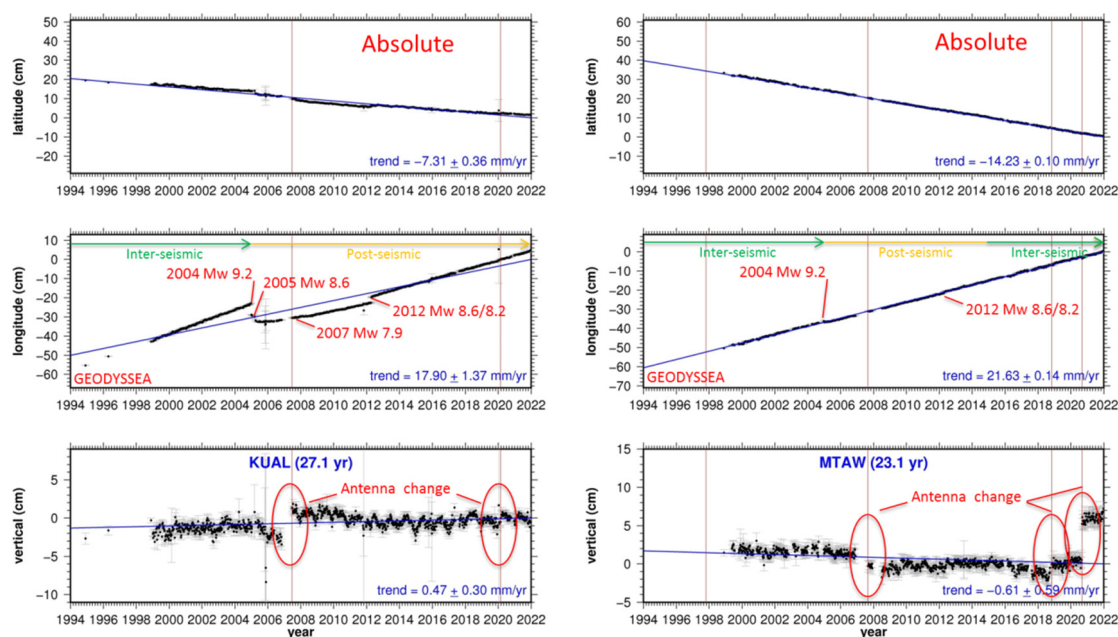

Figure 8. Unfiltered absolute 3D GPS position time series (1994–2021) for stations KUAL (Kuala Terengganu, Peninsular Malaysia) and MTAW (Tawau, Sabah, East Malaysia), with the 1994–1998 positions coming from the GEODYSSEA campaign measurements. In the longitude position figures, the major earthquake events that resulted in horizontal co-seismic position offsets are shown (2004 Mw 9.2 Sumatra–Andaman, 2005 Mw 8.6 Nias, 2007 Mw 7.9 Bengkulu, and 2012 Mw 8.6/8.2 Indian Ocean). Shown also (approximately) are the inter- (green) and post-seismic (yellow) phases of the 2004 Mw 9.2 Sumatra–Andaman earthquake. Antenna changes that have impacted the vertical position time series are also shown by red ellipses. Finally, the (raw) linear trend estimates are shown in blue.

Since the focus is on VLM, only equipment-related changes (e.g., a different antenna type and/or (wrong) antenna height) position jumps had to be estimated for the vertical position time series, as they are not affected by discontinuities due to any of the earthquake events. These have been estimated as relative (baseline) position jumps with re-

spect to the nearest (unaffected by an antenna change) station at each occurrence in the vertical position time series (additional information is provided and illustrated by Figure S7 in the Supplementary Materials) This also has the advantage that the entire horizontal (including the post-seismic (non-linear) part) position time series remains untouched versus when a 3D position jump (with respect to a linear trend line) is estimated (and thus remains identical for the horizontal directions as shown in Figure 8). Otherwise, artificial position jumps would be introduced in the horizontal post-seismic (2005-present) time series, especially for the Malaysian Peninsula. The velocity estimation was repeated until no vertical position jumps were present anymore.

Each 3D position jump estimate (Table S1 in the Supplementary Materials) was removed from all subsequent position solutions in the position time series. For the stations KUAL and MTAW, this is shown in Figure 9. In case of a station combination (e.g., TAWA-MTAW, GETI-GET2) or re-location (e.g., TGRH/SEMP), a tie was computed using either all overlapping weekly averaged positions or, otherwise, 12 weeks before and after a station re-location. Then, the estimated XYZ tie was applied to the initial station location, so that a continuous combined position time series was obtained.

The 3D position time series indicate that Peninsular Malaysia is still in the post-seismic phase of the 2004 Mw 9.2 earthquake (as for station KUAL in Figure 8), with horizontal motions still affected and lower than the inter-seismic motions that were recorded by the MASS stations from 1999 to 2004, with the NW of Peninsular Malaysia still affected the most. This is in agreement with what was observed for the south of Thailand by Simons et al. [5]. In East Malaysia, the horizontal motions were only briefly affected following the Mw 9.2 event, and no impact on the vertical motions was observed there. For Peninsular Malaysia, there, however, is a distinct difference for the VLM in the time periods 1994–2004 (slight tectonic uplift) and 2005–2021 (tectonic subsidence, which has been flattening out in recent years). The pattern looks very similar to a downscaled version of the VLM that was observed on the Island of Phuket in Thailand [5,25]. In Phuket, the co- and post-seismic motions are the highest, since it is located closer to the 2004 Mw 9.2 earthquake epicenter in the Sumatra trench.
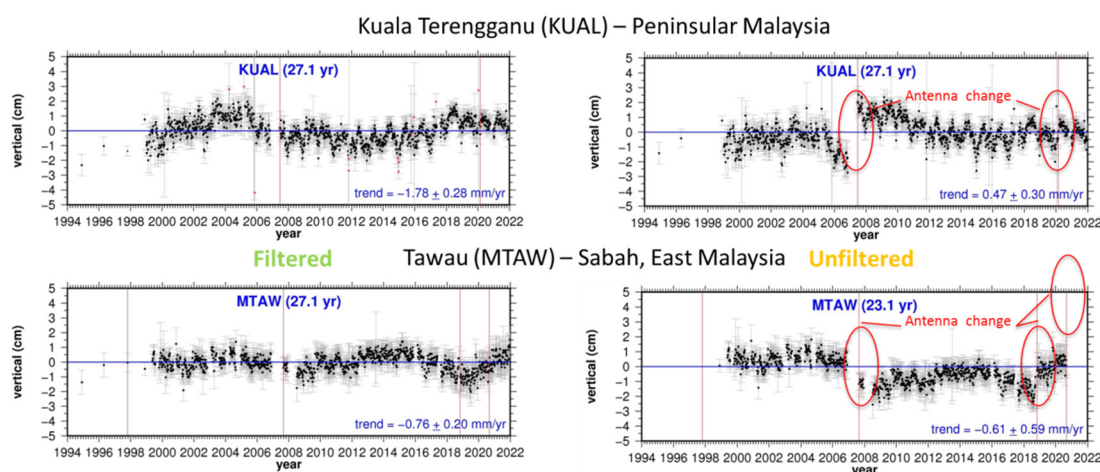

Figure 9. Filtered and unfiltered (detrended) vertical GPS position time series (1994–2021) for stations KUAL (Kuala Terengganu, Peninsular Malaysia) and MTAW (Tawau, Sabah, East Malaysia. The left panel shows the vertical position time series with all antenna-change-related position jumps removed. The single linear trend estimates are shown in blue.

Figure 10 shows the final VLM estimates for stations KUAL and MTAW with the seasonal variations modeled as $A \cos k \times (2\pi t + B)$, with A being the amplitude of the cosine, t the time in years, and B the phase shift in days after 1 January ($k \times 365.25$ days/360°, k being 1 and 0.5 for, resp., the annual and semi-annual cycle), whereby the parameters A and B have been estimated along with the linear regressions [36]. The estimates for all

locations in Peninsular Malaysia and East Malaysia are included as plots in the Supplementary Materials (Figures S5 and S6), and the results are summarized in Tables 6 and 7.
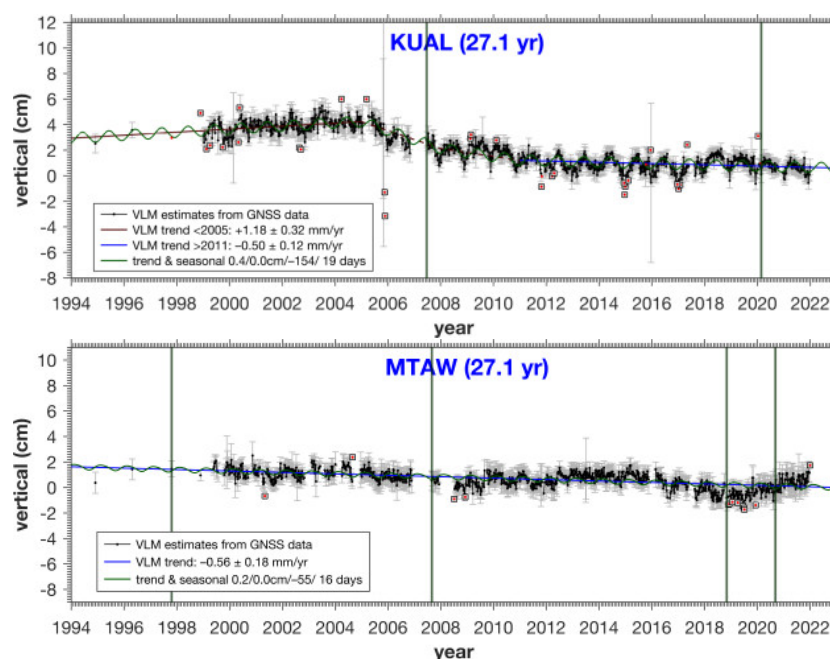

Figure 10. Vertical land motion estimates for KUAL in Peninsular Malaysia (split trend lines) and MTAW in Sabah, East Malaysia (single trend line) (1994–2021). For each station, the vertical position time series is given along with the total observation period. The reference vertical position is given on 1 January 2022 (0 cm). The green vertical lines are the epochs at which a vertical position jump (due to antenna change or MASS to MyRTKNet transition) was estimated. The linear trend lines are given in brown (<2005) and blue (>2011) with the modeled seasonal (annual) signal (green) superimposed on it. Weekly averaged position outliers are marked in red. The vertical land motion estimate is given at a 95% (1.96 sigma) confidence level. We chose to model the exponentially decaying signal after the Sumatra–Andaman Earthquake by 3 linear segments and only consider the part after 2011 to connect closest to the present-day situation.

Table 6. VLM trend estimates at 21 locations in Peninsular Malaysia and Singapore (1994–2021). At 10 locations, split trend estimates distinguish between the inter-seismic period until 25 December 2004 (<2005) and the post-seismic period (>2005, linear trend estimate from 2011 onwards) from 26 December 2004 onwards due to the 2004 Mw 9.2 Sumatra–Andaman earthquake. The red font indicates that the station is located nearby a Malaysian tide gauge and combined MASS/MyRTKNet stations are given as MASS+MRTK. The linear trend estimates are given at a 95% confidence level (1.96 sigma). The number of estimated (vertical) position jumps for each station is given, and also the amplitude and phase of the annual and semi-annual signals. The residual sigma is the SD of the difference between the data and the model fit.

Location	Station	Position Jumps	VLM Estimate (95% CL) Absolute (IGS14) (mm/year)		Annual (cm/days)	Semi-Annual (cm/days)	Residual SD (cm)
			<2005	>2005			
1	LGKW	3	-	−0.46 ± 0.13	0.48/−126	0.13/−75	0.37
2	ARAU	2	−0.17 ± 0.36	−1.14 ± 0.11	0.36/−103	0.09/−47	0.47
	UUMK	3	-	0.45 ± 0.13	0.40/−110	0.07/−73	0.41
3	GETI + GET2	4	0.40 ± 0.33	−2.73 ± 0.13	0.63/−151	0.08/−71	0.44
4	USMP	2	−1.37 ± 0.41	−0.79 ± 0.16	0.39/−96	0.11/−69	0.39
	BABH	4	-	−0.28 ± 0.13	0.39/−108	0.09/−57	0.31
5	GRIK	1	-	0.64 ± 0.13	0.35/−130	0.08/−43	0.42
6	PUPK	3	-	0.79 ± 0.14	0.30/−109	0.12/−60	0.36
7	GMUS	1	-	−0.45 ± 0.14	0.29/−137	0.02/38	0.39

Location	Station	Position Jumps	VLM Estimate (inter-seismic)	VLM Estimate (post-seismic)	Annual	Semi-Annual	Residual SD
8	KUAL	3	1.18 ± 0.32	−0.50 ± 0.12	0.41/−154	0.01/19	0.45
9	BEHR	5	−0.37 ± 1.13	−1.28 ± 0.16	0.34/−110	0.13/−51	0.37
10	MERU	1	-	−3.29 ± 0.13	0.34/−77	0.07/64	0.35
11	KTPK + UPMS	3	0.85 ± 0.30	−0.22 ± 0.13	0.34/−104	0.08/−74	0.32
12	TLOH	3	-	−0.19 ± 0.13	0.26/−128	0.08/−85	0.34
13	KUAN + PEKN	2	−1.06 ± 0.32	−1.14 ± 0.13	0.34/−148	0.02/85	0.36
14	JUML	2	-	−0.28 ± 0.13	0.26/−118	0.07/−62	0.32
15	SEGA+SEG1	2	1.06 ± 0.67	−1.54 ± 0.15	0.38/−105	0.02/4	0.46
16	MERS + MRSG	1	-	−0.11 ± 0.14	0.38/−159	0.06/−77	0.34
17	KUKP	2	-	−4.75 ± 0.15	0.25/−124	0.06/−40	0.35
18	TGRH + SDLI	2	-	−0.20 ± 0.13	0.30/−149	0.11/−43	0.32
19	TGPG	1	-	−0.55 ± 0.14	0.29/−139	0.07/−55	0.37
20	UTMJ + JHJY	4	1.75 ± 0.36	−1.18 ± 0.12	0.34/−138	0.11/−88	0.41
21	NTUS	2	0.72 ± 0.31	0.05 ± 0.15	0.41/−147	0.09/−62	0.38

Table 7. VLM trend estimates at 17 locations in East Malaysia and Northern Kalimantan (1994–2021). The red font indicates that the station is located nearby a Malaysian tide gauge and combined MASS/MyRTKNet stations are given as MASS+MRTK. The linear trend estimates are given at a 95% confidence level (1.96 sigma). The number of estimated (vertical) position jumps for each station is given, and also the amplitude and phase of the annual and semi-annual signals. The residual sigma is the SD of the difference between the data and the model fit.

Location	Station	Position Jumps	VLM Estimate (95% CL) Absolute (IGS14) (mm/year) 1994–2021	Annual (cm/days)	Semi-Annual (cm/days)	Residual SD (cm)
1	KUCH + UMAS	2	−0.66 ± 0.16	0.20/−147	0.06/−77	0.36
2	SIBU+SIB1	3	−0.97 ± 0.16	0.12/−111	0.04/79	0.33
3	BINT + BIN1	2	−1.13 ± 0.21	0.23/−86	0.08/78	0.47
4	MIRI	2	−0.63 ± 0.17	0.26/−99	0.04/78	0.38
5	LABU + LAB1	3	−1.48 ± 0.16	0.23/−97	0.03/59	0.36
6	KINA + UMSS	2	−1.86 ± 0.22	0.13/−90	0.05/−48	0.52
7	MKNB	1	−0.97 ± 0.48	0.24/−82	0.13/−83	0.41
8	KUDA	1	−0.19 ± 0.24	0.22/−81	0.02/9	0.34
9	MRDU	2	−5.88 ± 0.38	0.10/−130	0.02/−44	0.49
10	SAND	3	−1.05 ± 0.18	0.23/−81	0.08/75	0.42
11	DATU	1	0.51 ± 0.22	0.20/−79	0.03/−53	0.29
12	SEMP	2	−0.32 ± 0.21	0.18/−69	0.04/−33	0.28
13	TAWA + MTAW	4	−0.56 ± 0.18	0.20/−55	0.03/16	0.48
14	CNAT	0	0.31 ± 0.71	0.25/−154	0.07/−91	0.35
15	CBAS	0	−0.27 ± 0.72	0.28/−117	0.13/−80	0.51
16	CPUT	0	−0.73 ± 0.58	0.12/−30	0.09/87	0.41
17	CNAU	1	−2.04 ± 0.49	0.07/4	0.06/77	0.35

Peninsular Malaysia

In Table 6, two different types of vertical position time series can be distinguished. Those including MASS GPS data (ARAU, GET2, USMP, KUAL, BEHR, UPMS, PEKN, SEG1, JHJY, and NTUS) hence include vertical positions prior to the 2004 Mw 9.2 Sumatra–Andaman earthquake. The newer MyRTKNet stations came online in 2005. We split the trends before and after the 26 December 2004 earthquake for the locations where GPS stations were already operational in 1999. Hence, we can distinguish VLM in the inter-seismic (up to 25 December 2004) and post-seismic periods. This is of importance when validating the RSL from the TG results with VLM from GNSS as, at the majority of the stations, tectonic uplift precedes tectonic subsidence. Since we approximate the

post-seismic motion with a linear trend, we opted to model the exponentially decaying signal after the Sumatra–Andaman Earthquake [25] by 3 linear segments and only consider the part after 2011 to establish best the present-day VLM situation. The slope of the post-seismic motion has then already decreased significantly. All segments are connected without any vertical jumps.

The VLM results for Peninsular Malaysia indicate post-seismic tectonic subsidence that decreases as time progresses, similar to what was observed on Phuket Island [5], be it at lower rates. However, at a few locations, the vertical motion is a bit different: USMP (Penang) indicates land subsidence prior to 2005, similar to PEKN (mainly coming from the combination with the KUAN MASS station (Kuantan). Very significant are the high subsidence rates that are observed at MERU (−3.29 ± 0.13 mm/year) in Meru and KUKP (-4.75 ± 0.15 mm/year) at Kukup. Both appear to result from human-induced land subsidence due to groundwater extraction. Finally, a few stations indicate some slight uplift occurring after 2015 (e.g., UUMK, PUKP, JUML, and JHJY). For some stations (BEHR/TGPG), parts of the position time series were excluded from the trend estimations, as they suffered from GPS data and/or GNSS antenna (setup)-related issues in these periods (further details are given in Table S2 of the Supplementary Materials). Table 6 shows that at all 10 locations with split trends in Peninsular Malaysia, there was post-seismic tectonic subsidence after 2005, and with the exception of USMP and PEKN, the peninsula was subjected to tectonically induced uplift until the occurrence of the Mw 9.2 event in 2004 (again, similar to what was observed for Phuket). The RSL results from the TG data in Peninsular Malaysia in Section 3.1 were likewise estimated with split trends so that the RSL from the independent SALT–GNSS combination can be compared over similar data intervals (Section 4).

East Malaysia

The VLM results for East Malaysia and Northern Kalimantan, Indonesia in Table 7 look more stable and constant over the analyzed period. Most of the VLM rates are between −0.5 and −1.5 mm/year and no changes in patterns during the analyzed period are observed. Again, for some stations (SIB1/MIRI/LAB1/UMSS/KUDA), parts of the position time series were excluded from the trend estimations, as they suffered from GPS data and/or GNSS antenna (setup)-related issues in these periods (further details are given in Table S2 of the Supplementary Materials). For station UMSS, issues with the tilting of the GNSS monument also occurred (at least) between 2006 and 2008. In East Malaysia, there is also one location that experienced substantial land subsidence (MRDU −5.90 ± 0.38 mm/year) in Kota Marudu, Sabah. Moreover, one other station shows uplift (DATU 0.51 ± 0.23 mm/year) that may have resulted from active tectonics related to the accommodation of the (remaining) convergence between the Philippine Sea and Sundaland plates that is transferred through the Sulu ridge. The TU Delft station MKNB on Mount Kinabalu suggests that the mountain height is decreasing by −0.95 ± 0.50 mm/year, while, after the start of the measurements back in 2013, the VLM results initially indicated a slight annual increase in height before the Mw 6.0 earthquake occurred in September 2015. The time series of the four BIG stations (2014–2021) are still relatively short to already provide accurate VLM estimates, but station CNAT on the Riau/Natuna Islands should have a near-zero VLM estimate (0.29 ± 0.74 mm/year) since it is located near the core of the Sundaland plate with no known active tectonic processes.

Finally, the VLM results for Peninsular and East Malaysia are plotted in Figures 11 and 12. Figure 11 for the Peninsula shows both the inter- (1999–2004) and post-seismic (2005–2021) VLM estimates for stations that were operational already in 1999. At the majority of these stations, a clear change in VLM trend estimates can be observed (change from uplift (green arrows) to subsidence (red arrows).
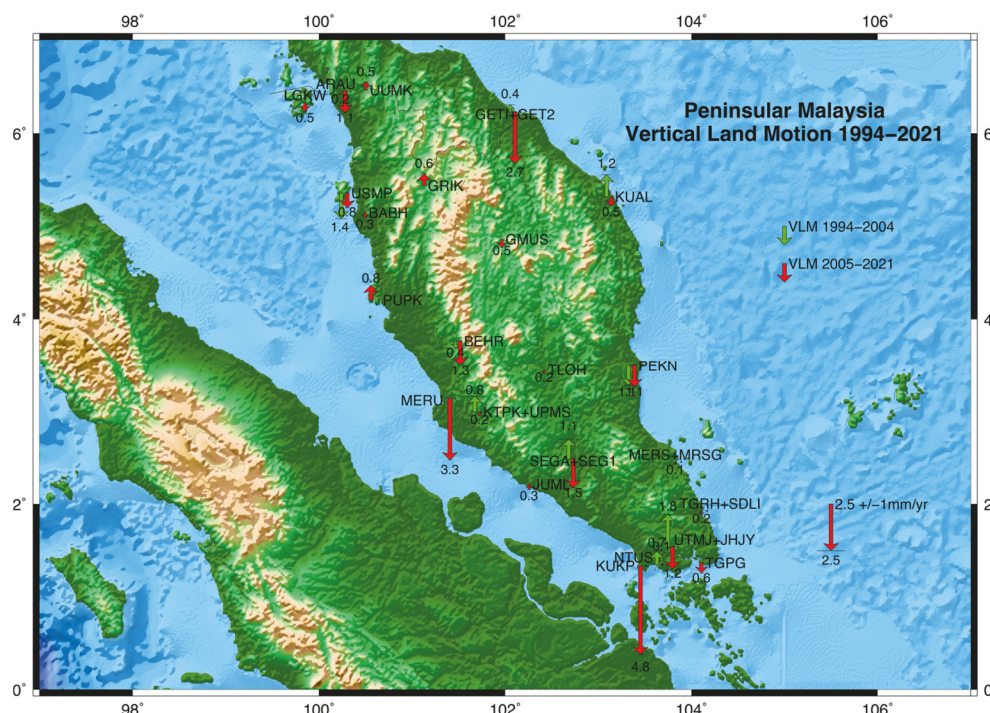
Figure 11. Vertical land motion estimates (1994–2021) in Peninsular Malaysia/Singapore. The estimates based on (split) trends (<2005 (green arrows) and >2005 (red arrows)) are shown for sites that were operational before 2005. The vertical land motion error estimates are given at a 95% confidence level. The *y*-axis is the latitude (N) and the *x*-axis is the longitude (E), both given in degrees.
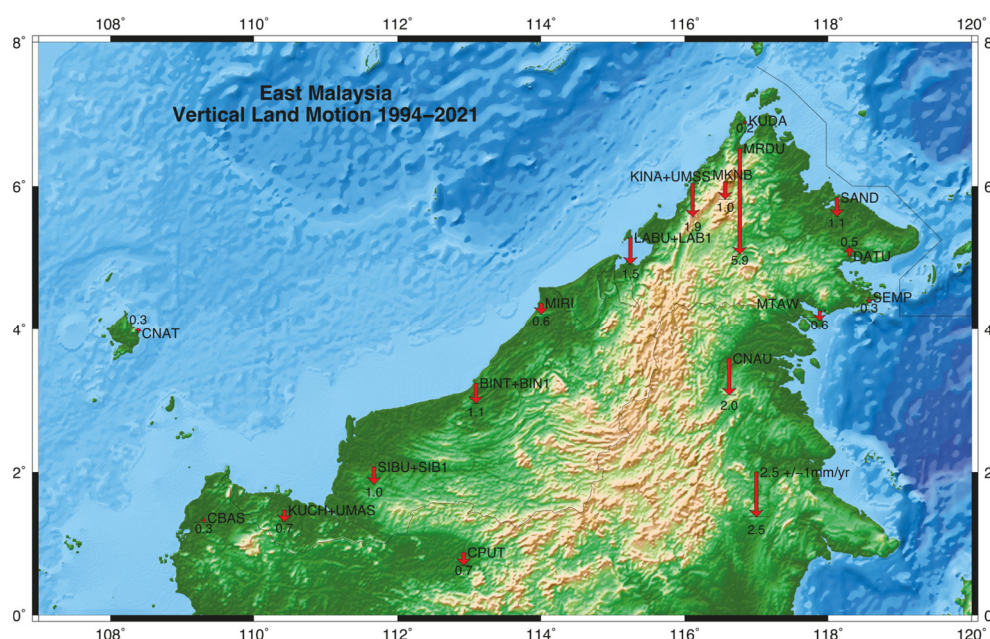

Figure 12. Vertical land motion estimates (1994–2021) in East Malaysia/Kalimantan given as a single VLM trend (1994–2021). The vertical land motion error estimates are given at a 95% confidence level. The *y*-axis is the latitude (N) and the *x*-axis is the longitude (E), both given in degrees.

It is, however, difficult to distinguish between VLM as a result of tectonic (inter- and post-seismic) processes and more local processes (e.g., groundwater variation) because no detailed information is available on the GNSS monumentation. If monuments are located on bedrock, they will only register VLM due to geophysical processes that vary only on a regional scale. If instead they are located on a sediment layer, then the pillar depth will determine how much VLM due to human-induced land subsidence is regis-

tered, as the GNSS observations only sense what occurs below their foundation. So, for example, the subsidence rate in Meru on the surface could be even higher if the MERU monument has a 10 m foundation depth. Knowledge of the foundation depth and geological composition of the ground layer is required to study the observed VLM motions in more detail. Nonetheless, it seems that the majority of Peninsular Malaysia has undergone tectonic land subsidence since the end of 2004 and experienced tectonic uplift previously. At some stations, this tectonic uplift/downfall signal might be masked due to local (land subsidence) processes. Moreover, TG benchmarks might have different foundation depths and hence the VLM registered by GNSS stations might not be affecting the TG benchmark in the same way. Therefore, it is recommended to co-locate GNSS with TG stations.

4. Results on Relative Sea-Level Rise

Human-induced or tectonically induced land subsidence, when combined with absolute sea-level rise, contributes to higher observed rates of relative sea-level rise along the coast. In a previous study [25], a good match between the RSL results from TG and the ASL–VLM combination from, respectively, SALT and GPS was observed for Phuket Island in Thailand. This study observed that the VLM (GPS) clearly shows linear tectonic uplift before the 2004 Mw 9.2 Sumatra–Andaman earthquake and non-linear (decaying) tectonic subsidence afterward that appears to flatten out after 2018. Moreover, TG clearly shows linear RSL until the end of 2004, followed by a period of non-linear RSL increase that mirrors the VLM. ASL from SALT shows a linear trend for the entire period since it is not affected by VLM.

In this section, we investigate how valid similar comparisons are for both Peninsular and East Malaysia and whether the TG results can be validated with the ASL–VLM combination. For Peninsular Malaysia, we compared the inter-seismic (1984–2004) and post-seismic (2005–2020) periods separately. Therefore, the TG trend estimations in Peninsular Malaysia have been split into two parts as discussed in Section 3.1, and the same applies to the VLM estimates for the combined MASS/MyRTKNet station locations (1999–2021) given in Section 3.3.

At five GNSS locations nearby TGs (GET, PEN, CHD, NKP, and JBH), split VLM trends are available, so the RSL can be compared over two time periods (before and after 2005). An example is given below in Figure 13, which shows comparisons for RSL estimates from the TG at Kuala Terengganu (CHD) with the difference in the ASL from SALT (near the TG station) and the VLM of station KUAL (located 8 km away). For TG station CHD, the RSL linear trend estimates (top panel Figure 13) are 2.90 ± 0.33 mm/year (<2005) and 4.46 ± 0.46 mm/year (>2005). The ASL estimate (a single value for the entire period since ASL is not affected by vertical ground motion) is 3.52 ± 0.24 mm/year (middle panel, Figure 13). The VLM linear trend estimates (bottom panel Figure 13) are 1.18 ± 0.32 mm/year (<2005) and −0.50 ± 0.12 mm/year (>2005). The independently estimated RSL trend estimates (ASL-VLM) are, therefore, 2.34 ± 0.40 mm/year (<2005) and 4.02 ± 0.27 mm/year (>2005). Both RSL values agree with the estimates from the TG data within 0.6 mm/year (<2005) and 0.4 mm/year (>2005). The good fit in the post-seismic period (>2005) was achieved by using only the last segment (after 2011) of the four-segment piecewise linear regression since in the first 6 years the (non-linear) decay of the tectonic subsidence signal was still significant. Both differences are well within their error boundaries (95% confidence level) and the RSL values in each period indicate that the use of one single trend estimate would not be suited to the analyzed time period for Peninsular Malaysia. The RSL comparisons for all TG locations in Peninsular Malaysia and East Malaysia are given, respectively, in Tables 8 and 9.
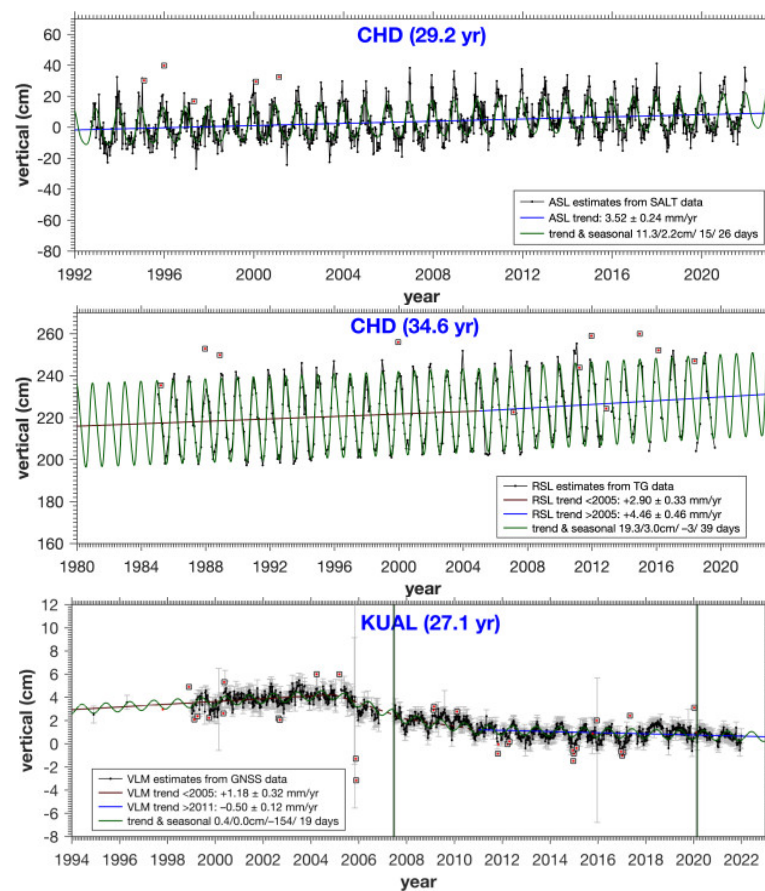
Figure 13. Relative sea level (from tide gauge), absolute sea level (from satellite altimetry), and vertical land motion (from GPS) trend estimates for tide-gauge station CHD and nearby GNSS station KUAL. The linear trend estimates from the tide gauges and GPS data have been split into two parts (<2005 and >2005).

For Peninsular Malaysia (Table 8), the best RSL comparison results in the inter-seismic period (<2005, values highlighted in blue) were achieved for TG stations CHD, GET, and JBH. The RSL estimate differences at PEN and NKP are still reasonable but might be affected by a different VLM at the TG and the nearest GNSS station. Both GNSS stations (USMP and PEKN (KUAN)) show subsidence during the inter-seismic period (<2005), while tectonic uplift was still occurring in Peninsular Malaysia. In the post-seismic period (>2005), the RSL (TG) and RSL (SALT−GNSS) are very similar. For TG location SED, the VLM estimate might not be representative of the TG location since it was estimated using the combination of GNSS stations TGRH and SDLI (the latter being operational since 2015 close to the TG location but 25 km away from TGRH). In Kukup and Meru, the TGs (KUK and, more so, PTK) seem to be subsiding less than the VLM estimated from the position time series of the nearby GNSS stations (KUKP and MERU). A different monumentation depth or locally varying subsidence rates could explain this. Overall, for Peninsular Malaysia, we observed for 10 out of 12 TG stations a good match between the in situ RSL from TG and the synthetic RSL from nearby VLM and ASL (SALT−GNSS), especially if we consider the period after 2005. Only the TG locations PTK and SED are the outliers.

Table 8. RSL comparison (TG versus SALT−VLM) for 12 locations in Peninsular Malaysia. Shown are the final ASL, VLM (from the nearest GNSS station), RSL (from TG), and RSL (from SALT−GNSS). For all TG locations, the RSL (TG) trend estimates were split (<2005 and >2005). For the VLM, this was only possible for TG locations GET, PEN, CHD, NKP, and PEN since no VLM data were available here before 2005. In blue and purple, the values to be compared are highlighted, which are either two periods (<2005 and >2005) or one period (>2005) for locations where the MyRTKNet stations only became operational after 2005. The distance from the TG to the nearest GNSS station is also given. All error estimates are given at a 95% confidence level (1.96 sigma).

TG Station	Nearest GNSS Station	Distance (km)	ASL (SALT) (mm/year) 1992–2020	VLM (GNSS) (mm/year)		RSL (TG) (mm/year)		RSL (SALT−GNSS) (mm/year)	
				<2005	>2005	<2005	>2005	<2005	>2005
LAN	LKGW	15	4.08 ± 0.28	-	−0.46 ± 0.13	2.23 ± 0.55	4.61 ± 0.69	-	4.54 ± 0.31
GET	GET2	0	3.68 ± 0.24	0.40 ± 0.33	−2.73 ± 0.13	2.70 ± 0.47	5.56 ± 0.67	3.28 ± 0.41	6.41 ± 0.27
PEN	USMP	8	4.03 ± 0.29	−1.37 ± 0.41	−0.79 ± 0.16	2.50 ± 0.51	4.80 ± 0.71	5.40 ± 0.50	4.82 ± 0.33
CHD	KUAL	8	3.52 ± 0.24	1.18 ± 0.32	−0.50 ± 0.12	2.90 ± 0.33	4.46 ± 0.46	2.34 ± 0.40	4.02 ± 0.27
LUM	PUPK	7	4.30 ± 0.31	-	0.79 ± 0.14	2.27 ± 0.50	3.60 ± 0.66	-	3.51 ± 0.34
NKP	PEKN	54	3.66 ± 0.26	−1.06 ± 0.32	−1.14 ± 0.13	2.56 ± 0.29	5.05 ± 0.42	4.72 ± 0.41	4.80 ± 0.29
PTK	MERU	11	4.73 ± 0.35	-	−3.29 ± 0.13	1.57 ± 0.50	3.66 ± 0.72	-	8.02 ± 0.37
TIO	MRSG	52	3.67 ± 0.27	-	−0.11 ± 0.14	2.18 ± 0.32	4.26 ± 0.40	-	3.78 ± 0.30
TGK	JUML	11	4.08 ± 0.27	-	−0.28 ± 0.13	1.69 ± 0.47	3.31 ± 0.64	-	4.36 ± 0.30
SED	SDLI	1	4.88 ± 0.29	-	−0.20 ± 0.13	2.23 ± 0.37	2.55 ± 0.45	-	5.08 ± 0.32
JBH	JHJY	8	5.12 ± 0.31	1.75 ± 0.36	−1.18 ± 0.12	2.13 ± 0.27	7.84 ± 0.61	3.37 ± 0.48	6.30 ± 0.33
KUK	KUKP	1	4.73 ± 0.34	-	−4.75 ± 0.15	1.87 ± 0.38	7.97 ± 0.48	-	9.48 ± 0.37

Table 9. RSL comparison (TG versus SALT−VLM) for 9 locations in East Malaysia. Shown are the final ASL, VLM (from the nearest GNSS station), RSL (from TG), and RSL (from SALT−GNSS). In blue and purple, the RSL values to be compared are highlighted. The distance from the TG to the nearest GNSS station is also given. All error estimates are given at a 95% confidence level (1.96 sigma).

TG Station	Nearest GNSS Station	Distance (km)	ASL (SALT) (mm/year) 1992–2020	VLM (GNSS) (mm/year) 1994–2021	RSL (TG) (mm/year) 1985–2019	RSL (SALT−GNSS) (mm/year) 1992–2021
KCH	UMAS	12	4.18 ± 0.19	−0.66 ± 0.16	−4.98 ± 0.34	4.84 ± 0.25 *
BTU	BIN1	4	3.43 ± 0.23	−1.13 ± 0.21	2.52 ± 0.28	4.56 ± 0.31 **
MYY	MIRI	4	3.66 ± 0.18	−0.63 ± 0.17	4.84 ± 0.31	4.29 ± 0.25 ***
LBU	LAB1	1	3.64 ± 0.27	−1.48 ± 0.16	2.08 ± 0.40	5.12 ± 0.31 **
KKB	UMSS	8	3.88 ± 0.24	−1.86 ± 0.22	3.82 ± 0.29	5.74 ± 0.33 **
KUD	KUDA	4	3.92 ± 0.22	−0.19 ± 0.24	2.46 ± 0.40	4.11 ± 0.33 **
SDK	SAND	7	4.34 ± 0.20	−1.05 ± 0.18	2.75 ± 0.36	5.39 ± 0.27 **
LDU	DATU	6	4.76 ± 0.20	0.51 ± 0.22	1.83 ± 0.47	4.25 ± 0.30 **
TWU	MTAW	3	4.49 ± 0.23	−0.56 ± 0.18	3.07 ± 0.34	5.05 ± 0.29 **

* The KCH TG station (Kuching) shows a very unrealistic behavior (RSL going down); here we opt to choose the synthetic RSL, which is more consistent with the surroundings. ** For all these stations, when we discard the TG data after 2014, the match between RSL from TG and synthetic RSL from SALT−GNSS improves considerably: on average, this adds an extra 2 to 3 mm/year to the TG RSL trend. *** For the MYY TG station (Miri), we introduced vertical jumps in the TG data to better fit the synthetic RSL from SALT−GNSS. These jumps are also obvious when inspecting the remaining signal after the initial fit (sigma): we applied a +82 cm jump before 1991 and a -10 cm jump after 2004.

For East Malaysia (Table 9), the RSLs from both independent methods are compared with linear trend estimates for the entire period (1987–2021), since no post-seismic vertical subsidence following the 2004 Mw 9.2 earthquake near Sumatra occurred here. The

two independent RSL estimates here typically only fit within 2 mm/year, with higher differences up to 3 mm/year for LBU/LAB1 and SDK/SAND. The observed differences are also beyond the error estimates (Table 9) obtained from both methods. A clear anomaly is KCH/UMAS in Kuching where the TG appears to register a sea-level fall of −4.98 ± 0.34 mm/year, while the SALT−VLM suggests an RSL of 4.84 ± 0.25 mm/year. The latter value seems more reliable, as the ASL trend means that the TG should otherwise have a positive VLM of ~9 mm/year in a region (West Sarawak) with no known active tectonic processes [24]. Generally, the synthetic TG (SALT−GNSS) values appear more consistent for East Malaysia.

It is possible to find a much better match for East Malaysia if the TG data after 2014 are excluded. The consistent deviation (RSL (TG) in Table 9) from what is expected hints at a problem in the TG data after 2014 for the whole of East Malaysia. As we found (undocumented) jumps in the TG data of the MIRI station, we introduced two jumps to better match the RSLs, so this one is a good fit, but that was intended. The TG station at Kuching behaves such that we do not trust its data. Whether this is just an error or is to be attributed to a local phenomenon is under investigation. In general, however, the ASL estimates are all higher than the RSL from the TGs and we do not observe any uplift in the VLMs along the coastline of East Malaysia. We therefore made two additional RSL comparisons for East Malaysia (Tables S3 and S4 in the Supplementary Materials), whereby, in the first comparison, we discarded all TG data after 2014 for East Malaysia. This leads, excluding KCH and MYY, to a better match (differences < 1.5 mm/year) between TG RSL and the synthetic SALT−GNSS RSL. In the second comparison, an even better result (differences < 0.5 mm/year) can be obtained by adding 6.5 cm to the data after 1 January 2014 for each of these TG stations, which is quite remarkable. Assuming an average rise of 5 mm/year, a similar result would be obtained by adding 5 cm after 2012.5 or 7 cm after 2015. Again, this needs further inquiries by the TG authorities.

Since there is no information available on the foundation depth and bottom geology on which both the TG and GNSS station benchmarks were constructed, it is difficult to state which of the two RSL estimation methods gives the most reliable estimate at each location. Therefore, it is also difficult to decide which of the independently determined RSL values should be plotted as the final RSL result. We suggest plotting both RSL values and discarding obvious outliers (such as RSL (TG) from KCH). For Peninsular Malaysia, the RSL values after 2005 might be the best choice as they represent the most recent RSL situation in the post-seismic VLM aftermath of the 2004 Mw 9.2 earthquake. Figure 14 shows a geographical representation of these choices. The bottom plot seems to be more consistent with current knowledge about relative sea-level rise and is also consistent with earlier predictions [37]. The VLM and RSL values (TG and SALT − GNSS) for Peninsular Malaysia (Table 8) cannot be directly compared with the most recent estimates of Din et al. [17], since our trend estimates were split (<2005 and >2005). Hence, our latest RSL estimates generally are lower and higher, respectively, before and after 2005 due to the inter-seismic uplift and post-seismic subsidence in these time periods. For East Malaysia, our RSL (TG 1985–2019) estimates (Table 9) are typically lower by 2–3 mm/year than those of Din et al. [17], with a TG data span from 1993 to 2011. However, very similar values can be observed in Tables S3 and S4, where we discarded or introduced and offset the TG data after 2014, which again points to a possible issue with the TG records after this date.
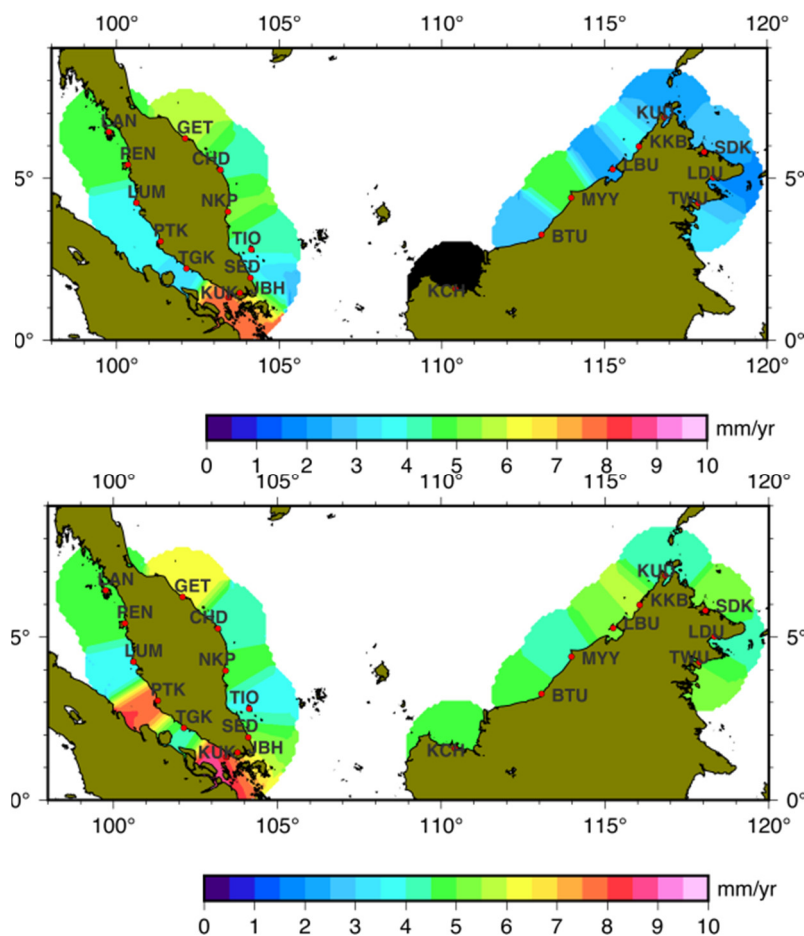
Figure 14. Relative sea-level rise estimates for Peninsular and East Malaysia. The top panel shows the relative sea-level rise from 12 and 9 tide-gauge trend estimates on, respectively, Peninsular (2005–2019) and East Malaysia (1985–2019). The bottom panel shows also the relative sea-level rise, now synthesized from SALT absolute sea-level rise minus GPS vertical land motion, for the same 21 tide-gauge locations in Peninsular (2005–2021) and East Malaysia (1992–2021). The black area in the top panel is due to the erroneous tide-gauge records at station KCH (Kuching), which suggest significant sea-level fall. The 2 red areas in the bottom panel are due to human-induced land subsidence of the GNSS stations in Meru and Kukup. The top panel indicates that this is not registered by the PTK tide gauge near Meru.

5. Conclusions

Relative sea level (RSL) trends have been estimated from TG data at 21 locations in Peninsular and East Malaysia. A robust RSL analysis and validation of results were carried out, whereby TG, SALT, and GNSS time series (starting from raw data) were combined using the same parameterization and trend estimation method rather than combining results from different (external) sources. A new approach was the splitting of the RSL linear trend estimates in Peninsular Malaysia into two parts to account for the inter- and post-seismic land behavior due to the 2004 Mw 9.2 Sumatra–Andaman earthquake. At all TG locations, the ASL linear trend estimates were also estimated from satellite altimetry (SALT) data.

MASS/MyRTKNet GPS data (1999–2021) from 47 stations (13 decommissioned and 34 active) were analyzed to estimate VLM (in IGS14) at 35 locations in both Peninsular and East Malaysia. This study optimally combined stations to obtain the longest possible position time series (max span: 1994–2021), whereby extensive attention was given to the removal of vertical position jumps due to antenna (set-up) changes. Along with modeling seasonal signals, this resulted in VLM uncertainties typically below 0.3 mm/year (95% confidence level).

VLM indicates (tectonic) that subsidence in Peninsular Malaysia was initiated by the 2004 Mw 9.2 Sumatra–Andaman earthquake, which has resulted (with a decaying rate) in a land fall of 3–5 cm in the past 17 years. In East Malaysia, subsidence rates are lower (−0.5 to −1.0 mm/year), with a total land fall of 2–3 cm in the same period. Three regions have significantly higher (human-induced) subsidence rates (−3 to −6 mm/year)—Kukup and Meru in Peninsular Malaysia and Kota Marudu in Sabah—indicating that these GNSS stations are not anchored to bedrock. Lahud Datu (in Sabah near the Sulu Arc) shows signs of tectonic uplift. A small number of VLM estimates might be less reliable due to either local vertical motion phenomena or monument instability (UMSS/SEG1).

As a first for Peninsular and East Malaysia, we adopted VLM estimates from GNSS and combined them with ASL trends from altimetry to validate the relative sea-level changes recorded at all available tide gauges. For Peninsular Malaysia, we find mostly good matches (RSL values within 1 mm/year) both in the inter- and post-seismic periods. For East Malaysia, the validation shows higher differences (2–3 mm/year) than for the study case in Phuket, South Thailand (slightly north of Peninsular Malaysia). This poorer match for East Malaysia is significantly improved by either not including data after 1 January 2014 or applying a generic jump to all East Malay TGs of +6.5 cm to the data after 1 January 2014. The combination of VLM and ASL estimates could also provide RSL estimates at additional coastal areas where no TG data are available.

In Peninsular Malaysia, the VLM changed (as in South Thailand) into a non-linear post-seismic pattern after 2005, making a single linear fit to both the entire TG and VLM time series not suitable. Splitting the linear fit here, also (like for Phuket Island), into an inter- and post-seismic part significantly improves the RSL validation for Peninsular Malaysia. TG results indicate a present RSL rise around Peninsular Malaysia of 3–5 mm/year (2005–2019) and in East Malaysia (no KCH) of 2–4 mm/year (1987–2019). SALT shows ASL rise (1992–2020) near Peninsular Malaysia at 3.5–5 mm/year and near East Malaysia at 3.5–4.5 mm/year. VLM shows tectonic subsidence in Peninsular Malaysia (excluding MERU/KUKP) up to −2 mm/year (2011–2021) and East Malaysia (no MRDU/UMSS/DATU) up to −1 mm/year (1998–2021). All these estimates come with uncertainties, whereby, in general, VLM is considered to be the most reliable, as after the model fits, the sigma of the residual VLM data is one order of magnitude lower than that of the RSL and ASL data. VLM from GNSS and VLM at TGs are compatible if they have the same foundation (depths) (ideal: both located on bedrock). VLM and TG linear estimates are compatible over a given period if no pattern (e.g., land uplift to land fall/linear to non-linear) changes occurred during this period. SALT is not affected by the VLM.

It is not known how representative the VLM (from GPS) is for the nearby TG locations, as little information is known about the foundation type/depth and geology at both locations. Distances are often also more than 5–10 km. The co-location of GNSS at TGs is therefore highly recommended.

Author Contributions: Conceptualization, W.S., M.N. and M.K.; methodology, W.S. and M.N.; tide-gauge and satellite altimetry trends determination, M.N.; vertical land motions, W.S., A.M. and J.E.; validation, M.N. and W.S.; formal analysis, M.N. and W.S.; writing—original draft preparation, W.S., M.N., A.M. and P.N.; writing—review and editing W.S., M.N., M.K., P.N. and A.H.D.; supervision W.S., M.K., Z.G., W.D.R. and S.C. All authors have read and agreed to the published version of the manuscript.

Conflicts of Interest: The authors declare no conflict of interest.

Abbreviations

ASEAN	Association of Southeast Asian Nations
ASL	Absolute Sea Level
BIG	Geospatial Information Agency (formerly known as BAKOSURTANAL)
DSMM	Department Survey and Mapping Malaysia
EU	European Union
EUMETSAT	European Organisation for the Exploitation of Meteorological Satellites
GEODYSSEA	Geodynamics of South and South East Asia
GIA	Glacial Isostatic Adjustment
GNSS	Global Navigation Satellite System
GPS	Global Positioning System
GIPSY-OASIS	GNSS-Inferred Positioning System and Orbit Analysis Simulation Software
IERS	International Earth Rotation and Reference Systems Service
IGS	International GNSS Service
InaCORS	Indonesian Continuously Operating Reference Station
IOD	Indian Ocean Dipole
ITRF	International Terrestrial Reference Frame
JPL	Jet Propulsion Laboratory
LRM	Low-Resolution Mode
MASS	Malaysian Active GPS System
MSL	Mean Sea Level
Mw	Moment Magnitude
MyRTKNet	Malaysia Real-Time Kinematic GNSS Network
NNR	No Net Rotation
NOAA	National Oceanic and Atmospheric Administration
NWO	Dutch Research Council
PPP	Precise Point Positioning
PS InSAR	Persistent Scatterer Interferometric Synthetic Aperture Radar
PSMSL	Permanent Service for Mean Sea Level
RADS	Radar Altimeter Database System
RSL	Relative Sea Level
SALT	Satellite Altimetry

SLA	Sea Level Anomaly
TG	Tide Gauge
TUDelft	Delft University of Technology
VLM	Vertical Land Motion
WGS84	World Geodetic System 1984
WRMS	Weighted Root Mean Square
yr	year (mm/yr = mm/year)

References

1. White, N.J. Coastal and global averaged sea level rise for 1950 to 2000. *Geophys. Res. Lett.* **2005**, *32*, L01601. https://doi.org/10.1029/2004GL021391.
2. Tang, K.H.D. Climate change in Malaysia: Trends, contributors, impacts, mitigation and adaptations. *Sci. Total Environ.* **2019**, *650*, 1858–1871. https://doi.org/10.1016/j.scitotenv.2018.09.316.
3. Bagheri, M.; Ibrahim, Z.Z.; Akhir, M.F.; Oryani, B.; Rezania, S.; Wolf, I.D.; Pour, A.B.; Talaat, W.I.A.W. Impacts of Future Sea-Level Rise under Global Warming Assessed from Tide Gauge Records: A Case Study of the East Coast Economic Region of Peninsular Malaysia. *Land* **2021**, *10*, 1382. https://doi.org/10.3390/land10121382.
4. Sarkar, M.S.K.; Begum, R.A.; Pereira, J.J.; Jaafar, A.H.; Saari, M.Y. Impacts of and Adaptations to Sea Level Rise in Malaysia. *Asian J. Water Environ.* **2014**, *11*, 29–36.
5. Kamaruddin, A.H.; Din, A.H.M.; Pa'suya, M.F.; Omar, K.M. Long-term sea level trend from tidal data in Malaysia. In Proceedings of the 2016 7th IEEE Control and System Graduate Research Colloquium (ICSGRC), Shah Alam, Malaysia, 8 August 2016; pp. 187–192.
6. Simons, W.J.F.; Naeije, M.C.; Brown, B.E.; Niemnil, S.; Pradit, S.; Thongtham, N.; Mustafar, M.A.; Towatana, P.; Darnsawasdi, R.; Yucharoen, M.; et al. Vertical motion of Phuket Island (1994–2018) due to the Sumatra-Andaman mega-thrust earthquake cycle: Impact on sea-level and consequences for coral reefs. *Mar. Geol.* **2019**, *414*, 92–102. https://doi.org/10.1016/j.margeo.2019.05.008.
7. Kowalczyk, K.; Pajak, K.; Wieczorek, B.; Naumowicz, B. An Analysis of Vertical Crustal Movements along the European Coast from Satellite Altimetry, Tide Gauge, GNSS and Radar Interferometry. *Remote Sens.* **2021**, *13*, 2173. https://doi.org/10.3390/rs13112173.
8. Klos, A.; Kusche, J.; Fenoglio-Marc, L.; Bos, M.S.; Bogusz, J. Introducing a vertical land motion model for improving estimates of sea level rates derived from tide gauge records affected by earthquakes. *GPS Solut.* **2019**, *23*, 102. https://doi.org/10.1007/s10291-019-0896-1.
9. Harvey, T.C.; Hamlington, B.D.; Frederikse, T.; Nerem, R.S.; Piecuch, C.G.; Hammond, W.C.; Blewitt, G.; Thompson, P.R.; Bekaert, D.P.S.; Landerer, F.W.; et al. Ocean mass, sterodynamic effects, and vertical land motion largely explain US coast relative sea level rise. *Commun. Earth Environ.* **2021**, *2*, 233. https://doi.org/10.1038/s43247-021-00300-w.
10. Din, A.H.M.; Reba, M.N.M.; Omar, K.M.; Ses, S.; Latip, A.S.A. Monitoring Vertical Land Motion in Malaysia Using Global Positioning System (GPS). In Proceedings of the the 36th Asian Conference on Remote Sensing (ACRS), Quezon City, Philippines, 19–23 October, 2015; p. 11.
11. Azhari, M.; Altamimi, Z.; Azman, G.; Kadir, M.; Simons, W.J.F.; Sohaime, R.; Yunus, M.Y.; Irwan, M.J.; Asyran, C.A.; Soeb, N.; et al. Semi-kinematic geodetic reference frame based on the ITRF2014 for Malaysia. *J. Geod. Sci.* **2020**, *10*, 91–109. https://doi.org/10.1515/jogs-2020-0108.
12. Satirapod, C.; Trisirisatayawong, I.; Fleitout, L.; Garaud, J.D.; Simons, W.J.F. Vertical motions in Thailand after the 2004 Sumatra–Andaman Earthquake from GPS observations and its geophysical modelling. *Adv. Space Res.* **2013**, *51*, 1565–1571. https://doi.org/10.1016/j.asr.2012.04.030.
13. Vigny, C.; Simons, W.J.F.; Abu, S.; Bamphenyu, R.; Satirapod, C.; Choosakul, N.; Subarya, C.; Socquet, A.; Omar, K.; Abidin, H.Z.; et al. Insight into the 2004 Sumatra–Andaman earthquake from GPS measurements in southeast Asia. *Nature* **2005**, *436*, 201–206. https://doi.org/10.1038/nature03937.
14. Luu, Q.H.; Tkalich, P.; Tay, T.W. Sea level trend and variability around Peninsular Malaysia. *Ocean Sci.* **2015**, *11*, 617–628. https://doi.org/10.5194/os-11-617-2015.
15. Hamid, A.I.A.; Din, A.H.M.; Hwang, C.; Khalid, N.F.; Tugi, A.; Omar, K.M. Contemporary sea level rise rates around Malaysia: Altimeter data optimization for assessing coastal impact. *J. Asian Earth Sci.* **2018**, *166*, 247–259. https://doi.org/10.1016/j.jseaes.2018.07.034.
16. Hamid, A.I.A.; Din, A.H.M.; Khalid, N.F.; Omar, K.M. Acceleration of Sea Level Rise over Malaysian Seas from Satellite Altimeter. *Int. Arch. Photogramm.* **2016**, *42*, 277. https://doi.org/10.5194/isprs-archives-XLII-4-W1-277-2016.
17. Din, A.H.M.; Zulkifli, N.A.; Hamden, M.H.; Aris, W.A.W. Sea level trend over Malaysian seas from multi-mission satellite altimetry and vertical land motion corrected tidal data. *Adv. Space Res.* **2019**, *63*, 3452–3472. https://doi.org/10.1016/j.asr.2019.02.022.
18. Cob, S.; Kadir, M.; Forsberg, R.; Simons, W.; Naeije, M.; Din, A.H.; Yacob, H.; Amat, A.; Mahdzur, D.; Ibrahim, Z.; et al. Epoch-Based Height Reference System for Sea Level Rise Impact Assessment on the Coast of Peninsular Malaysia. *Remote Sens.* **2022**, *14*, 6179. https://doi.org/10.3390/rs14236179.

19. Hamilton, W.B. *Tectonics of the Indonesian Region*; US Government Printing Office（USGS）: Washington, DC, USA, 1979; Volume 1078.https://doi.org/10.3133/pp1078
20. Simons, W.J.F.; Socquet, A.; Vigny, C.; Ambrosius, B.A.C.; Haji Abu, S.; Promthong, C.; Subarya, C.; Sarsito, D.A.; Matheussen, S.; Morgan, P.; et al. A decade of GPS in Southeast Asia: Resolving Sundaland motion and boundaries. *J. Geophys. Res.* **2007**, *112*, B06420. https://doi.org/10.1029/2005JB003868.
21. Satirapod, C.; Simons, W.; Promthong, C.; Yousamran, S.; Trisirisatayawong, I. Deformation of Thailand as Detected by GPS Measurements due to the December 26th, 2004 Mega-Thrust Earthquake. *Surv. Rev.* **2007**, *39*, 109–115. https://doi.org/10.1179/003962607X165069.
22. Bird, P. An updated digital model of plate boundaries. *Geochem. Geophys. Geosys.* **2003**, *4*. https://doi.org/10.1029/2001GC000252.
23. Argus, D.F.; Gordon, R.G.; DeMets, C. Geologically current motion of 56 plates relative to the no-net-rotation reference frame. *Geochem. Geophys. Geosys.* **2011**, *12*, 1–13. https://doi.org/10.1029/2011GC003751.
24. Mustafar, M.A.; Simons, W.J.F.; Tongkul, F.; Satirapod, C.; Omar, K.M.; Visser, P.N.A.M. Quantifying deformation in North Borneo with GPS. *J. Geod.* **2017**, *91*, 1241–1259. https://doi.org/10.1007/s00190-017-1024-z.
25. Naeije, M.C.; Simons, W.J.F.; Pradit, S.; Niemnil, S.; Thongtham, N.; Mustafar, M.A.; Noppradit, P. Monitoring Megathrust-Earthquake-Cycle-Induced Relative Sea-Level Changes near Phuket, South Thailand, Using (Space) Geodetic Techniques. *Remote Sens.* **2022**, *14*, 5145. https://doi.org/10.3390/rs14205145.
26. Webster, P.J.; Moore, A.M.; Loschnigg, J.P.; Leben, R.R. Coupled ocean–atmosphere dynamics in the Indian Ocean during 1997–98. *Nature* **1999**, *401*, 356–360. https://doi.org/10.1038/43848.
27. Saji, N.H.; Goswami, B.N.; Vinayachandran, P.N.; Yamagata, T. A dipole mode in the tropical Indian Ocean. *Nature* **1999**, *401*, 360–363. https://doi.org/10.1038/43854.
28. Wöppelmann, G.; Marcos, M. Vertical land motion as a key to understanding sea level change and variability. *Rev. Geophys.* **2016**, *54*, 64–92. https://doi.org/10.1002/2015RG000502.
29. Trisirisatayawong, I.; Naeije, M.; Simons, W.; Fenoglio-Marc, L. Sea level change in the Gulf of Thailand from GPS-corrected tide gauge data and multi-satellite altimetry. *Glob. Planet. Change* **2011**, *76*, 137–151. https://doi.org/10.1016/j.gloplacha.2010.12.010.
30. Scharroo, R.; Leuliette, E.; Lillibridge, J.; Byrne, D.; Naeije, M.; Mitchum, G. RADS: Consistent Multi-Mission Products. In Proceedings of the 20 Years of Progress in Radar Altimatry, Venice, Italy, 24–29 September 2012; p. 69.
31. Wilson, P.; Rais, J.; Reigber, C.; Reinhart, E.; Ambrosius, B.A.C.; Le Pichon, X.; Kasser, M.; Suharto, P.; Majid, D.A.; Yaakub, D.; et al. Study provides data on active plate tectonics in southeast Asia region. *Eos Trans. Am. Geophys. Union* **1998**, *79*, 545. https://doi.org/10.1029/98EO00398.
32. Jet Propulsion Laboratory. GNSS-Inferred Positioning System and Orbit Analysis Simulation Software (GIPSY-OASIS). Available online: https://gipsy-oasis.jpl.nasa.gov (accessed on 1 November 2019).
33. Rebischung, P.; Schmid, R. IGS14/igs14.atx: A new framework for the IGS products. In Proceedings of the AGU Fall Meeting, San Francisco, CA, USA, 14 December 2016.
34. Altamimi, Z.; Rebischung, P.; Métivier, L.; Collilieux, X. ITRF2014: A new release of the International Terrestrial Reference Frame modeling nonlinear station motions. *J. Geophys. Res. Solid Earth* **2016**, *121*, 6109–6131. https://doi.org/10.1002/2016JB013098.
35. Bertiger, W.; Desai, S.D.; Haines, B.; Harvey, N.; Moore, A.W.; Owen, S.; Weiss, J.P. Single receiver phase ambiguity resolution with GPS data. *J. Geod.* **2010**, *84*, 327–337. https://doi.org/10.1007/s00190-010-0371-9.
36. Blewitt, G.; Lavallée, D. Effect of annual signals on geodetic velocity. *J. Geophys. Res. Solid Earth* **2002**, *107*, ETG 9-1–ETG 9-11. https://doi.org/10.1029/2001JB000570.
37. Ercan, A.; Bin Mohamad, M.F.; Kavvas, M.L. The impact of climate change on sea level rise at Peninsular Malaysia and Sabah-Sarawak. *Hydrol. Processes* **2013**, *27*, 367–377. https://doi.org/10.1002/hyp.9232.